NAVAL POSTGRADUATE SCHOOL
Monterey, California

THESIS

AIR-SEA INTERACTIONS AND DEEP CONVECTION IN THE LABRADOR SEA

by

Laura S. Bramson

December, 1997

Thesis Co-Advisors: Peter Guest
Roland Garwood

Approved for public release; distribution is unlimited.

REPORT DOCUMENTATION PAGE

Form Approved OMB No. 0704-0188

1. AGENCY USE ONLY *(Leave blank)*	2. REPORT DATE	3. REPORT TYPE AND DATES COVERED
	December, 1997	Master's Thesis

4. TITLE AND SUBTITLE AIR-SEA INTERACTIONS AND DEEP CONVECTION IN THE LABRADOR SEA	5. FUNDING NUMBERS
6. AUTHOR(S) Laura S. Bramson	
7. PERFORMING ORGANIZATION NAME(S) AND ADDRESS(ES) Naval Postgraduate School Monterey CA 93943-5000	8. PERFORMING ORGANIZATION REPORT NUMBER
9. SPONSORING/MONITORING AGENCY NAME(S) AND ADDRESS(ES)	10. SPONSORING/MONITORING AGENCY REPORT NUMBER

11. SUPPLEMENTARY NOTES The views expressed in this thesis are those of the author and do not reflect the official policy or position of the Department of Defense or the U.S. Government.

12a. DISTRIBUTION/AVAILABILITY STATEMENT	12b. DISTRIBUTION CODE
Approved for public release; distribution is unlimited.	

13. ABSTRACT *(maximum 200 words)*

Deep convection in the oceans, particularly at high latitudes, plays an important role in the climate systems of the world's oceans and atmosphere. This study was conducted to examine atmospheric forcing effects on deep convection in the Labrador Sea. The Naval Postgraduate School one dimensional ocean mixed layer model was applied to the Labrador Sea from February 12 to March 10, 1997. The model was initialized and forced with oceanographic and atmospheric data collected onboard the R/V Knorr during the first field program of the Labrador Sea Deep Convection Experiment. An ocean mixed layer depth close to 1300 m was predicted and verified using the observed data. A sensitivity study was conducted using deviations from observations as input to determine how variations in atmospheric forcing could lead to the observed and even deepened ocean mixed layer. Observed Conductivity, temperature and depth (CTD) data were used to verify the model's spatial and temporal predictions of mixed layer temperature, salinity and depth. Model predicted mixed layer depths were usually slightly deeper than those observed. The final model output predicted temperature rather accurately, but model predicted salinity values were consistently low. A variety of sensitivity studies gave new insight to the individual influences of surface fluxes, momentum stresses, precipitation, salinity and individual storm variations to the mixed layer temperature, salinity and depth of the Labrador Sea.

14. SUBJECT TERMS	Labrador Sea Deep Ocean Convection Air-Sea Interactions	15. NUMBER OF PAGES 87
		16. PRICE CODE

17. SECURITY CLASSIFICATION OF REPORT	18. SECURITY CLASSIFICATION OF THIS PAGE	19. SECURITY CLASSIFICATION OF ABSTRACT	20. LIMITATION OF ABSTRACT
Unclassified	Unclassified	Unclassified	UL

NSN 7540-01-280-5500

Standard Form 298 (Rev. 2-89)
Prescribed by ANSI Std. 239-18 298-102

Approved for public release; distribution is unlimited.

AIR-SEA INTERACTIONS AND DEEP CONVECTION IN THE LABRADOR SEA

Laura S. Bramson
Lieutenant Commander, United States Navy
B.S., University of Miami, 1988

Submitted in partial fulfillment
of the requirements for the degree of

MASTER OF SCIENCE IN METEOROLOGY
MASTER OF SCIENCE IN PHYSICAL OCEANOGRAPHY

from the

NAVAL POSTGRADUATE SCHOOL
December 1997

Author: _____
Laura S. Bramson

Approved by: _____
Peter Guest, Thesis Co-Advisor

_____
Roland Garwood, Thesis Co-Advisor

_____
Carlyle H. Wash, Chairman
Department of Meteorology

_____
Robert Bourke, Chairman
Department of Oceanography

ABSTRACT

Deep convection in the oceans, particularly at high latitudes, plays an important role in the climate system of the world's oceans and atmosphere. This study was conducted to examine atmospheric forcing effects on deep convection in the Labrador Sea. The Naval Postgraduate School one dimensional ocean mixed layer model was applied to the Labrador Sea from February 12 to March 10, 1997. The model was initialized and forced with oceanographic and atmospheric data collected onboard the R/V Knorr during the initial phase of the Labrador Sea Deep Convection Experiment. An ocean mixed layer depth close to 1300 m was predicted and verified using the observed data. A sensitivity study was conducted using deviations from observations as input to determine how variations in atmospheric forcing could lead to the observed and deepened ocean mixed layer. Observed Conductivity, temperature and depth (CTD) data were used to verify the model's spatial and temporal predictions of mixed layer temperature, salinity and depth. Model mixed layer depths were usually slightly deeper than those observed. The final model output predicted temperature rather accurately, but model predicted salinity values were consistently low. A variety of sensitivity studies gave new insight to individual influences of surface fluxes, momentum stresses, precipitation, salinity and individual storm variations to the mixed layer temperature, salinity and depth of the Labrador Sea.

TABLE OF CONTENTS

ACKNOWLEDGMENTS

The Labrador Sea Deep Convection Experiment was sponsored by the Office of Naval Research programs on High Latitude Dynamics and Ocean Modeling and Prediction. My advisors, Dr. Guest and Dr. Garwood were supported by grants N0001497WR30058 and N0001496WR30051. The captain and crew of the R/V Knorr made possible a successful field program despite difficult environmental conditions. The meteorology measurement program on the Knorr was a collaborative effort by Peter Guest, NPS, Karl Bumke, Hauke Berndt, Uwe Karger and Klaus Uhlig, University of Kiel, Germany, and Fred Dobson and Bob Anderson, Bedford Institute of Oceanography, Nova Scotia.

I would like to thank both Dr. Garwood and Dr. Guest for their encouragement and assistance throughout this thesis study and Ms. Arlene Guest, without whom, many aspects of this thesis would have never gotten off the ground. Finally, I would like to thank my husband, John, whose patience and understanding were never ending.

I. INTRODUCTION

The Labrador Sea is an area of interest for oceanographers because this is a region where deep ocean convection leads to deep water formation. Deep ocean convection is a cold season phenomenon that causes the transfer of heat from the oceans' depth and the mixing of carbon dioxide from the oceans' surface. Schmitt (1996) noted that deep convection is closely related to large scale climate changes as it causes the warmer water of the ocean to release heat into the atmosphere thus acting as a basic mechanism to the earth's climate system. The atmosphere, through various air-sea interactions, is believed to play a key role in this process. The actual convection associated with deep water formation only occurs within small localized areas at relatively few locations in the world. In the northern hemisphere, Killworth (1983) found the main regions of deep water formation to be in the Labrador, Greenland, Iceland and Norwegian Seas. This deep water formation then circulates throughout the Atlantic to affect not just the area of origin but the entire basin. The details of this convective process and the subsequent deep water formation are still not fully understood.

Much of the present knowledge of the detailed process of deep convection is due to results from the laboratory and numerical experiments as wintertime data collection in these areas is difficult, and actual deep convection events are probably highly intermittent in space and time. The purpose of this study is to examine the physics of deep convection in the Labrador Sea. This was accomplished by applying the Naval Postgraduate School one dimensional ocean mixed layer model (Garwood, 1977, 1991) to the Labrador Sea. Initialization and verification data were collected onboard the R/V Knorr from February 2 to March 10, 1997 during the Labrador Sea Deep Convection Experiment.

A variety of air-sea interactions will be analyzed to gain an understanding of the ocean mixed layer conditions and changes. Conductivity, temperature and depth (CTD) measurements of February 12, February 25 and March 10, 1997 will be utilized to study the mixed layer temperature, salinity and depth as active convection occurred. Hypothetical

model predictions will be conducted to give insight to the mixed layer depth sensitivity to various parameters and demonstrate how very deep mixing could be possible.

Chapter II summarizes the meteorology and oceanography of the Labrador Sea and deep convection. A basic model description including the derivation of some of the major equations, instrumentation information, data calculations and assumptions utilized are described in Chapter III. More detailed information of the oceanographic and meteorological data collected along with general cruise conditions in the Labrador Sea are described in Chapter IV. Chapter V first describes the integrated ocean heat and salt loss with comparisons to measured surface heat fluxes. Then the various model integrations and predictions using the actual time dependent data are described including hypothetical cases to show possible variations to the mixed layer depth. Finally, Chapter VI summarizes the results making conclusions and recommendations for further applications and studies. Integral equation variables and constants are described in the appendix.

II. BACKGROUND

At high latitudes, the cooling and salinization of surface waters can cause them to sink to great depths. The cold, dense water then spreads away from the formation sites and renews the intermediate, deep and bottom waters of the world's oceans. This is an essential process in the thermohaline circulation of the oceans (Bunker and Worthington, 1976; Schmitz and McCartney, 1993). This type of deep convection only occurs in limited areas representing 1/1000 to 1/100 of the total surface of the global oceans (Gascard, 1990). However, at least 3/4 of the total volume of the world ocean must go through this process in order to renew deep waters every 1000 years (Broecker and Peng, 1982). One such area where this regularly occurs is in the Labrador Sea.

A. LABRADOR SEA DEEP CONVECTION EXPERIMENT

The Office of Naval Research established an Accelerated Research Initiative on Deep Oceanic Convection. The objective of this initiative, the Labrador Sea Deep Convection Experiment, is to improve the understanding of the convective dynamics of the ocean and thereby improve the parameterized representation of the convection in large-scale models. The objective is to be accomplished through a combination of meteorological and oceanographic field observations, laboratory studies, theory and numerical models. The initial field phase was successfully carried out by nineteen scientists from seven institutions onboard the R/V Knorr from February 2 to March 20, 1997.

B. LABRADOR SEA

1. Oceanography

The Labrador Sea is located south of the Davis Strait between the Canadian east coast and Greenland; it is bounded by a variety of currents (Fig 2.1). The West Greenland Current flows northward and westward off the Greenland coast carrying the warm, saline water of the East Greenland Current. The cold, fresh Labrador Current flows southward off Baffin Island and Labrador carrying water from Baffin Bay and the sounds of Baffin Island. Remnants of the very warm, saline Gulf Stream, the North Atlantic Current, flow off the

Nova Scotian continental shelf coming into contact with the Labrador Current on the Tail of the Banks off the Grand Banks of Newfoundland (Fairbridge,1966).

Numerous studies have reported that salinity and other water properties within the Labrador Sea have exhibited considerable interannual as well as annual variability (Lazier and Wright, 1993). Coastal waters form narrow belts of low salinity water on the continental shelves of both Greenland and Labrador. The water properties are not similar, however, as the Labrador shelf has much colder temperatures even throughout the summer. Clarke and Gascard (1983) noted that by the end of January most of the Labrador shelf is covered with ice due to the cold temperature and low salinity water. Throughout the winter months, this ice edge is almost continuous throughout the western and northern region of the sea leaving only the southwestern Greenland coast and the central gyre ice free (Fig 2.2).

Lazier (1980) describes the center of the Labrador Sea, away from the boundary currents, as having a slow, generally cyclonic circulation. Here the water mass in the top thousand meters is a mixture of cold, fresh polar water and warmer, saltier Atlantic water. During winter, the convective sinking of the surface water mixes the water and leads to formation of a distinct intermediate water type known as Labrador Sea Water (LSW). This water flows south into the Atlantic and can be traced almost to the Antarctic Ocean.

2. Meteorology

The climate of the Labrador Sea varies with location. The Canadian side is polar, continental while the Greenland side is polar, maritime. The annual mean air temperatures are approximately 5 - 7°C higher on the Greenland side at similar latitudes. The Canadian side has a larger mean annual range of air temperatures. Additionally, annual precipitation varies due to the maritime and continental differences as annual precipitation south of Cape Farwell reaches ~1000 mm while less than 250 mm of precipitation falls north of 55°N on the Canadian side. (Fairbridge,1966)

Both synoptic and mesoscale weather systems affect this region. On the synoptic scale, westerly winds dominate at high latitudes. Curry and McCartney (1996) noted that the strength of these westerlies, which blow the cold, dry air from Canada across the Labrador Basin, are a significant factor in determining the depth of the wintertime oceanic

convection. An increase in wind strength will remove more heat from the surface waters and deepen the extent of the convection. Also, large mesoscale phenomena such as polar lows which often form south of ice edges can cause a significant increase in the wind speed and surface fluxes. Each of these processes can significantly affect the air-sea temperature differences and the momentum stresses leading to strong air-sea interactions and consequently deepened convection of both the oceanic and atmospheric mixed layers.

C. DEEP CONVECTION

Schmitt (1996) describes deep convection as the key component of the ocean's role in Earth's climate. Strong winter cooling of northern surface waters causes heat to be transferred from the warmer ocean to the colder atmosphere. Due to the cooling of the water and brine rejection associated with ice formation, this water becomes denser than that below allowing the sinking and mixing of the surface water with deeper water. Schmitt (1996) believes that deep convection contributes to northern Europe's moderate winter climate.

The Labrador Sea has deep, convective overturning resulting primarily from winter cooling (Pickard and Emery, 1990). Lazier (1980) expected to find the most intense deep convection close to the Labrador slope where heat loss associated with the cold continental winds is most intense and the water column is least stable. These properties are likely to be found on the offshore side of the Labrador Current where the continental slope is coincident with the ice edge. Here, the meteorological forcing includes intense cooling and evaporation at the surface. Clarke and Gascard (1983) found that it is along this ice edge where the heat and water vapor fluxes from the ocean to the atmosphere in the Labrador Sea are greatest. More specifically, they found that the large cyclonic circulation preconditions deep convection by upwelling isopycnal surfaces at its center, thus reducing the overall vertical stability. Subsurface T-S maxima around the periphery of the circulation, when incorporated into the deepening mixed layer, then increase the water's density by increasing its salinity in addition to lowering its temperature.

Deep convection in the Labrador Sea is basically controlled by two mechanisms: the amount of summer warming and freshening versus the amount of winter cooling. Lazier (1980) has noted that deep convection does not occur every year. A decrease in salinity

during the summer due to the advection of low salinity water from the Labrador Current toward the east sometimes opposes the large heat loss. This low salinity water is thought to be a combination of fresh water runoff and melting of ice flowing through the Hudson Bay and Davis Strait. Lazier (1980) believes that this lower salinity water can increase the vertical stability and limit the winter convection to the top 100 to 200 m rather than the expected 400 to 1000 m during mild winters.

D. ATMOSPHERIC FORCING EFFECTS ON DEEP CONVECTION

Several theories have been proposed for how and why deep convection occurs. These theories have not been proven due to a sparsity of verification data. Collecting data in high latitude areas in the wintertime can pose unique problems. The Labrador Sea Deep Convection Experiment was an attempt to answer some of these questions.

It is known that strong atmospheric forcing, that is, strong surface fluxes and wind stresses, must be present in conjunction with other conditions for deep convection to occur (Kraus and Businger, 1994). For surface waters to sink to abyssal depths, they must not only be exposed to intense surface cooling but must also be preconditioned by a relatively high salinity to sink before freezing. The integrated heat and salinity fluxes are vitally important components to this process because they determine the overall static stability of the upper ocean. Short term wind stress and buoyancy fluxes are also important as they generate turbulent kinetic energy (TKE) that causes mixing and leads to entrainment and deepening of the mixed layer.

Although developments have been made in determining the important processes controlling deep convection, there are still many questions. One such question concerns the role of individual storms. Although it is simple to say that individual synoptic or mesoscale events of the atmosphere have an impact, it is still difficult to quantify the effect of the individual storm on oceanic deep convection. Theories associated with ocean plumes and chimney events are also major areas of study today as models attempt to predict the fully turbulent evolution of the oceanic flow fields. Whether these ocean plumes occur continuously, once a month, once a year or every few years is still under investigation. By attempting to explain some general characteristics of the Labrador Sea through the modeling

of individual events, one goal of this thesis is to obtain a better understanding of the atmospheric effects on deep convection.

Figure 2.1: The Labrador Sea and adjacent seas, currents and straits (from Lazier, 1980).

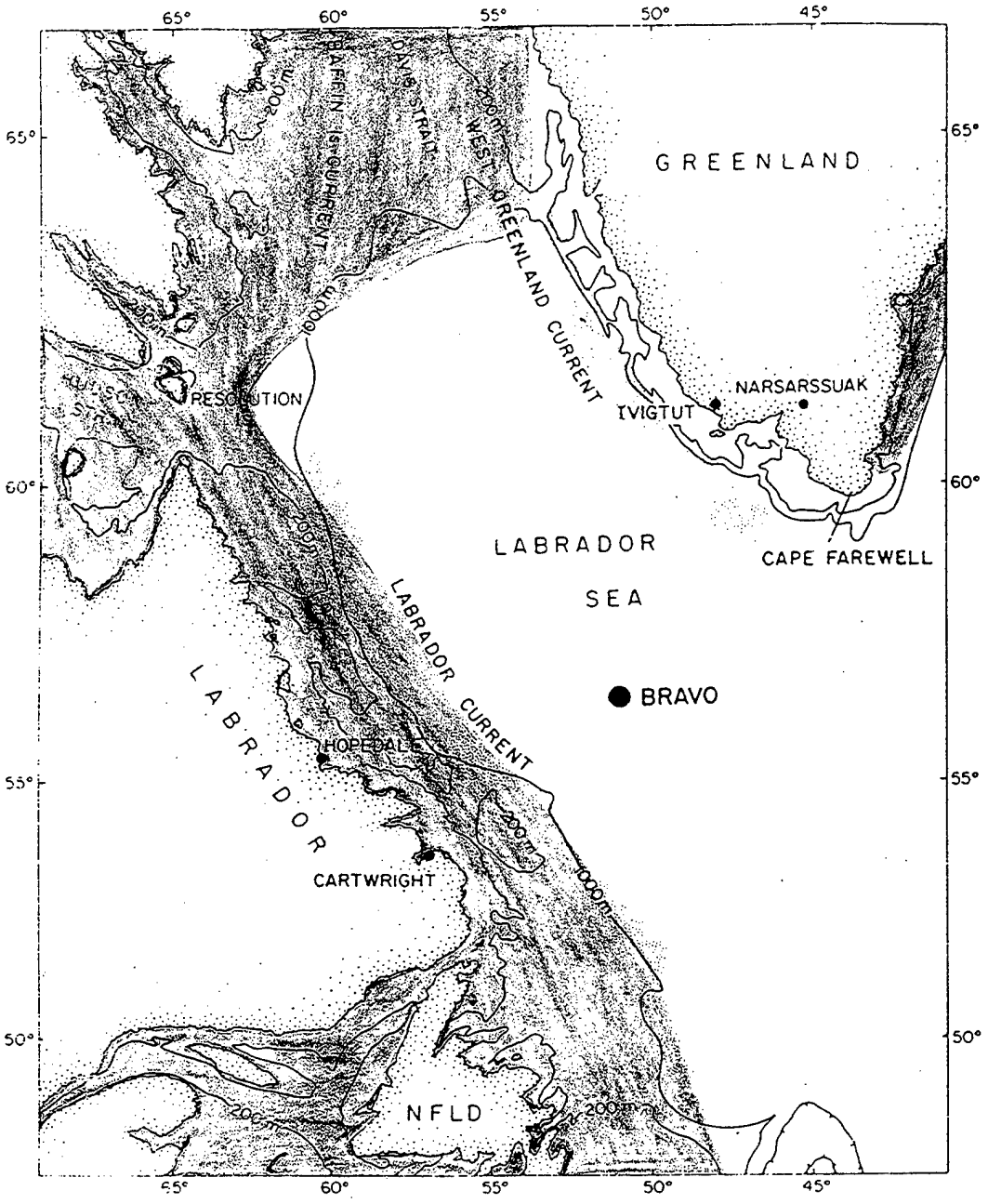

Figure 2.2: The Labrador Sea and mean ice edge (shown in blue) for March 1997. The central Labrador Sea remains ice free as the ice edge extends outward from the Labrador coast encompassing most of the Davis and Hudson Straits. The warm waters of the West Greenland Current allow most of the west coast of Greenland to remain ice free (modified from Lazier, 1980).

III. PROCEDURE

A. NAVAL POSTGRADUATE SCHOOL (NPS) 1-D OCEAN MIXED LAYER MODEL

1. Ocean Mixed Layer Structure

Garwood (1977) defines the ocean mixed layer to be the fully turbulent region of the upper ocean bounded above by the air-sea interface and below by a dynamically stable water mass. The source of energy for the generation of this turbulence is provided by the fluxes of heat, salt and momentum through the surface, as minimal vertical fluxes exist below the mixed layer.

The mixed layer is assumed to be homogeneous with relatively uniform temperature and salinity throughout. Directly below the mixed layer lies the turbulent entrainment zone, where both temperature and salinity undergo 'jump' conditions giving rise to strong gradients. Finally, below the entrainment zone, the water mass is stratified as density increases with depth.

2. 1-D Ocean Mixed Layer Model

The NPS mixed layer model is a one-dimensional ocean mixed layer model which uses a bulk second-order turbulence closure scheme. It includes a finite-thickness entrainment zone, both vertical and horizontal components of planetary rotation (Garwood et al., 1985) and thermobaric enhancement of entrainment (Garwood, 1991). It is a closed system of the three TKE equations computing all components of the in-situ turbulence. The governing equations are obtained by integration of the primitive equations over the depth of the mixed layer.

Garwood (1977) assumes that the turbulence of the overlying mixed layer provides the energy needed to destabilize and erode the underlying water mass leading to the TKE budget as the basis for the entrainment hypothesis. The one-dimensional total TKE equation is:

$$\frac{\partial}{\partial t}\left[\frac{\overline{u'^2+v'^2+w'^2}}{2}\right] = -\left[\overline{u'w'}\frac{\partial \bar{u}}{\partial z} + \overline{v'w'}\frac{\partial \bar{v}}{\partial z}\right] + \left[\alpha g\overline{T'w'} - \beta g\overline{S'w'}\right]$$

$$-\frac{\partial}{\partial t}\left[\overline{w'(\frac{p'}{\rho_o} + \frac{u'^2+v'^2+w'^2}{2})}\right] - \epsilon \qquad (3.1)$$

where: u, v, and w are the easterly, northerly and upward velocities, respectively.
The terms of the equation from left to right are:

(1) storage/time rate of change of TKE,

(2) shear production,

(3) buoyancy flux or damping of vertical turbulence,

(4) vertical diffusion by turbulent and pressure transport,

(5) viscous dissipation.

The linearized equation of state is utilized to express the buoyancy flux in terms of heat and salinity fluxes:

$$\rho = \rho_o[1 - \alpha(T - T_o) + \beta(S - S_o)] \qquad (3.2)$$

In polar latitudes the thermal expansion coefficient is very small. This leads to salinity, more specifically evaporation and precipitation, often dominating the buoyancy flux, contrary to midlatitude conditions. The buoyancy flux is defined as:

$$\overline{b'w'} = \alpha g\overline{T'w'} - \beta g\overline{S'w'} \qquad (3.3)$$

where α is the thermal expansion coefficient and β is the salinity "contraction" coefficient.

a. Entrainment

Within the entrainment zone, shear production and viscous dissipation are very small and considered negligible. The storage of TKE is then only dependent on the buoyancy flux and the turbulent/pressure transport. The 'jump' condition at the bottom of the entrainment zone for any conserved quantity, C, can be described by:

$$-\overline{C'w'}(-h) = w_e \Delta C \tag{3.4}$$

where ΔC is the mixed layer value minus the value below the entrainment zone.

This introduces the entrainment velocity, w_e. One goal is to predict entrainment at the mixed layer depth. Entrainment velocity can be described by the equation for the mixed layer depth:

$$\frac{\partial h}{\partial t} = w_e - w(-h) \tag{3.5}$$

Assuming no vertical motion, w(-h)=0, the equation becomes:

$$w_e = \frac{\partial h}{\partial t} \tag{3.6}$$

That is, with no upwelling or downwelling, deepening of the mixed layer is only due to entrainment.

b. Temperature and Salinity

Wind stress at the air-sea interface produces turbulence in the surface layer which is altered, transported and ultimately viscously dissipated. This turbulence causes the mixing which deepens the mixed layer and mixes temperature and salinity between the surface and the entrainment zone (Livezey, 1988).

First, conservation of heat requires:

$$\frac{\partial T}{\partial t} = -\frac{\partial \overline{T'w'}}{\partial z} \tag{3.7}$$

Next, the temperature flux at the surface can be defined as:

$$\overline{T'w'} = -\frac{Q_o}{\rho c_p} \tag{3.8}$$

where the net downward surface heat flux is:

$$Q_o = Q_{solar} - Q_{\substack{back \\ radiation}} - Q_{\substack{latent \\ heat}} - Q_{\substack{sensible \\ heat}} \tag{3.9}$$

Finally, the vertical integration of the temperature flux across the entrainment zone and then over the entire mixed layer leads to an equation defining the change in mixed layer temperature with respect to time:

$$\frac{\partial \overline{T}}{\partial t} = \frac{Q_o}{\rho c_p h} - \frac{\Delta \overline{T} w_e}{h} \tag{3.10}$$

Similarly, the same principles can be applied to the salinity budget:

$$\frac{\partial S}{\partial t} = -\frac{\partial \overline{S'w'}}{\partial z} \tag{3.11}$$

The surface salinity flux in polar seas is dependent not only on evaporation (E) and precipitation (P) but also on the freezing (F) and melting (μ) of ice:

$$\overline{S'w'} = -[E - P - \epsilon_1 (F - \mu)\overline{S}] \tag{3.12}$$

Likewise, the vertical integration across the entrainment zone and then over the entire mixed layer leads to an equation defining the change in mixed layer salinity with respect to time:

$$\frac{\partial \bar{S}}{\partial t} = \frac{[E - P + \epsilon_1 (F - \mu)\bar{S}]}{h} - \frac{\Delta \bar{S} w_e}{h} \tag{3.13}$$

To close the system of equations, the entrainment velocity is calculated by the vertical integration of the TKE budget under steady state conditions (i.e., the change of TKE with respect to time is negligible). The entrainment velocity becomes:

$$w_e = \frac{(\overline{w'^2})^{1/2} E}{\alpha g \Delta T - \beta g \Delta S} \tag{3.14}$$

where

$$E = \overline{u'^2 + v'^2 + w'^2} \tag{3.15}$$

This gives a system of equations for the mixed layer which can then be solved.

B. DATA

1. Bulk Method

The net density fluxes across the ocean's surface can be determined by the energy transferred by sensible and latent heat, evaporation minus precipitation, and the net radiation balance. In order to determine these surface fluxes of heat and the momentum stresses impressed upon an area, bulk parameterization methods are often employed. Smith (1988) showed that wind measurements taken from anemometers at different heights must be adjusted to a common reference height, usually 10 m, before they can be compared and used for surface forcing. This procedure is a convenient and consistent method of adjusting wind measurements to a common height and of finding bulk coefficients for wind stress and heat flux at the sea surface.

The wind speed, air and sea temperatures and specific humidities are each determined by measurements extrapolated to a reference height. The bulk transfer coefficients are determined by empirical relationships depending on surface roughness and stratification (i.e., surface layer stability). Given values of the bulk transfer coefficients, the wind stress, heat

flux and rate of evaporation in the atmospheric surface layer can then be estimated utilizing the following equations (Smith, 1988):

The drag coefficient is defined as:

$$c_D = \frac{\tau}{\rho_{air} u^2} \tag{3.16}$$

The heat flux coefficient is defined as:

$$c_T = \frac{Q_H}{\rho_{air} c_{pa} u (T_{sfc} - \theta)} \tag{3.17}$$

The evaporation coefficient is defined as:

$$c_E = \frac{Q_E}{\rho_{air} u (q_{sfc} - q)} \tag{3.18}$$

Numerous studies have shown that the drag coefficient , c_D, becomes larger at higher wind speeds due to a rougher sea surface. Based on the formula of Charnock (1955), Smith (1988) determined a roughness length scale, z_o, by adding the roughness length associated with a smooth surface to the roughness generated by wind stress. The resulting z_o can then be used along with empirical stability functions to determine c_D, and hence wind stress. Smith's (1988) neutral drag coefficients increased from about 1×10^{-3} at wind speeds from 2 to 5 m/s to 2×10^{-3} at 24 m/s.

Likewise, Smith (1988) defined a heat flux coefficient in near-neutral conditions. The heat flux coefficient was found to be nearly independent of wind speed; that is, it is essentially unaffected by surface roughness. He found that vertical density gradients can add or remove vertical kinetic energy, and thus affect the turbulent viscosity and diffusivity of mean properties required to support the corresponding vertical fluxes. Using the Monin-Obukhov stability, Smith (1988) used the heat flux coefficient, c_T, to describe both sensible heat flux and evaporation if humidity is only a minor contributor to stratification. Smith's

(1988) neutral heat flux coefficient is 1 x 10^{-3} while the neutral evaporation coefficient is 1.2 x 10^{-3}.

2. Labrador Sea Deep Convection Experiment

a. Data Collection

During the Labrador Sea Deep Convection Experiment a variety of meteorological and oceanographic studies were carried out. Scientists from Canada, Germany and the United States were able to collect data sets that represent the most complete of their kind for this region.

Despite mild conditions during December and the early portion of January, the latter part of the winter included sufficiently strong atmospheric forcing to not only erode the fresh, surface layer but give rise to oceanic convection down to 1500 m. Although it was desired to sample as much of the Labrador Sea as possible, observations in some locations were restricted due to the ice conditions. On the western side of the Labrador Sea the ice-pack extension from the shelf limited ship access.

Surface and meteorological data collected included latitude, longitude, ship speed, pressure, air temperature, dewpoint and intake (sea surface) temperature, relative humidity, relative and true wind speed, relative and true wind direction, ship speed and course, and ship position heading. Radiation data collected included downward shortwave radiation along with upward and downward longwave radiation. This enabled the calculation of overall net radiation, net shortwave and net longwave radiation. All data were based on 15 second samples averaged over five minute periods. Surface fluxes were then calculated utilizing the bulk parameterization method previously described. For the various model cases, the data was subsequently averaged over the period of an hour unless otherwise specified.

b. Ship Instrumentation

One goal of this project was to observe and characterize the thermodynamic and dynamic structure of the atmosphere. Rawinsondes were launched approximately six times per day. Two hundred and seventeen atmospheric profiles were collected successfully.

For better interpretation of the in-situ measurements, visual synoptic weather observations were recorded daily.

Three independent systems were utilized to measure shortwave and longwave components of downward surface radiation. Sea surface temperature was measured via infrared radiance and engine intake ports. Accurate radiance measurements were possible only about 75% of the time due to sea-spray and snow accumulation despite daily instrument cleanings. With cloudy conditions most of the cruise, the upward loss of heat due to net longwave radiation and surface warming from shortwave radiation was limited.

The air-sea flux measurements were made using an anemometer, a thermistor, and a hydrometer located at a height of 23 m. Other devices onboard the ship included a sonic anemometer, a fast-response propeller anemometer, two fast-response thermistors and a fast-response propeller anemometer. Also operated were a ceilometer, a 3 gHz vertical looking precipitation radar for ETL/NOAA and a moisture-flux sensor. The ETL/NOAA bow mast system, mounted aft on top of the hangar, measured incoming solar shortwave radiation, longwave radiation, turbulent winds with a sonic anemometer, precipitation via an optical disdrometer, ship's motion at the sensor site (top of bow mast), and separate gyrocompass and GPS signals.

For the oceanographic studies, hydrographic stations were chosen to obtain basin-wide coverage. All stations had CTD casts to the bottom and almost half included sampling of CFCs. Over 140 XBT's were dropped both on and between stations. Numerous drifters and floats were deployed throughout the 34 days which included RAFOS, Deep Lagrangian, VCM-PALACE, NSF-PALACE and ISF-PALACE floats, and WOTAN and BAROMETER drifters.

3. Conductivity Temperature Depth (CTD) Measurements

Three of the CTD station soundings were taken at 57.03° N and 53.92° W on February 12, February 25 and March 10, 1997, respectively. This location, with a water depth of almost 3500 m was away from the boundary currents in a region of high surface fluxes, and it was near the region of deepest observed convection. Here the water column was assumed to be approximately one dimensional with little advection. Plots of the

temperature and salinity CTD data showed an increasing mixed layer depth with time (Fig 3.1 and Fig 3.2). Each sounding contained the pressure, in-situ temperature, salinity, and dissolved oxygen. Below the mixed layer depths, the in-situ temperatures of each sounding were closely matched, confirming the one dimensional nature. The salinity values had very similar variations below the mixed layer, but the 12 February salinity cast was offset to significantly higher values when compared to the other two soundings. Because the second and third soundings showed agreement in salinity, it was concluded that the conductivity cell was not properly calibrated for the first sounding. A simple negative shift of the salinity profile was first attempted but did not correct the problem to satisfaction. A linear least square regression with depth as the independent variable was used to match the 12 February cast with the other two casts below the mixed layer. The correction was first applied to the pair of soundings from 12 to 25 February, then to the 12 February to 10 March pair. Because these gave two different corrections, an average of the two was used in the final application. The correction was then extended into the mixed layer as it was applied to the entire 12 February cast (Fig 3.2). Subsequent density profiles of the entire water column which included the corrected salinity values showed the expected homogeneous mixed layer and deep water stratification. The 12 February corrected salinity profile was used for all model integrations and experiments.

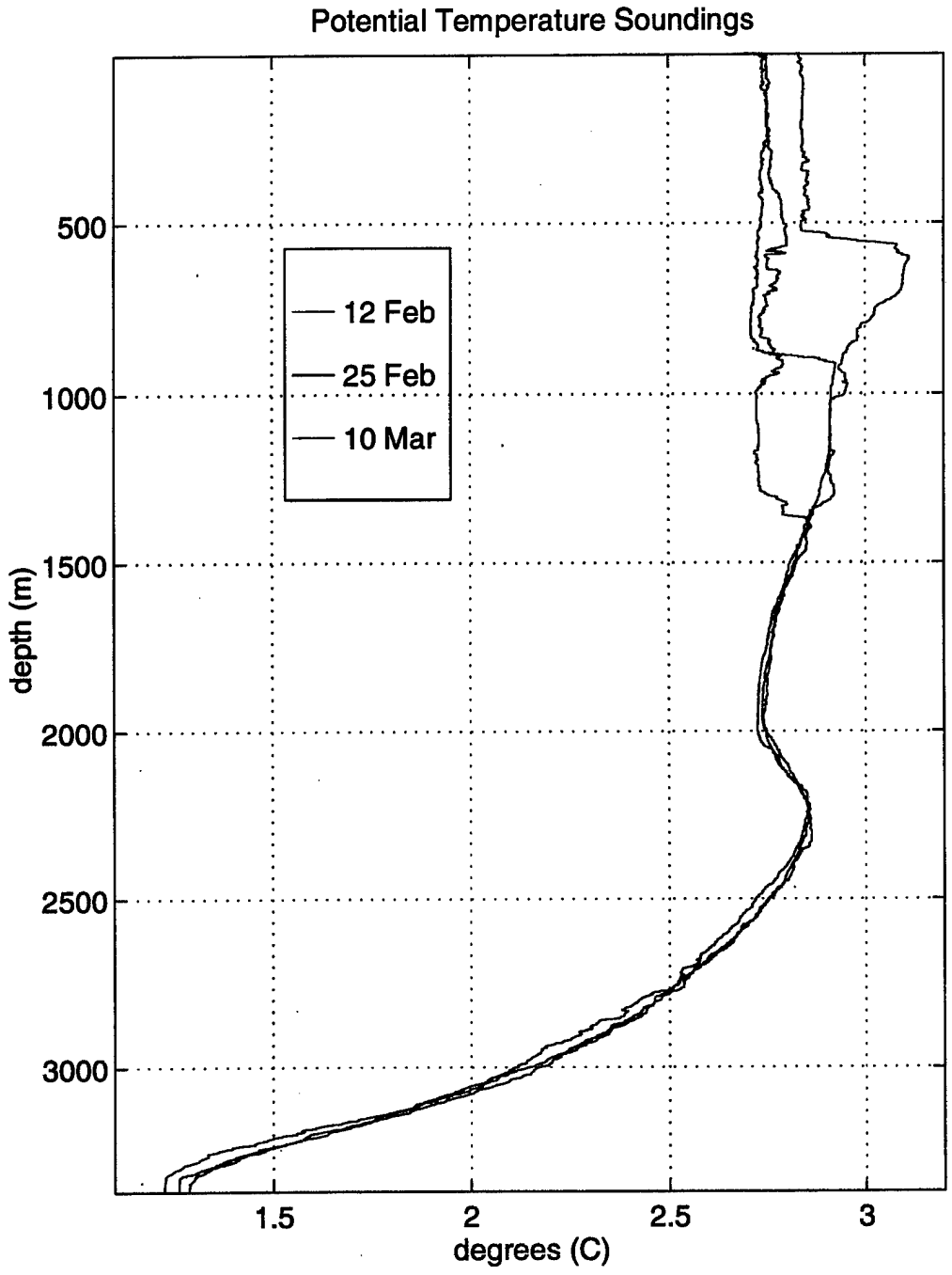

Figure 3.1: Observed potential temperature soundings for February 12, February 25 and March 10, 1997 at 57°N and 54°W. Note the mixed layer depth increased from 525 m, to 875 m, and finally to 1285 m, respectively.

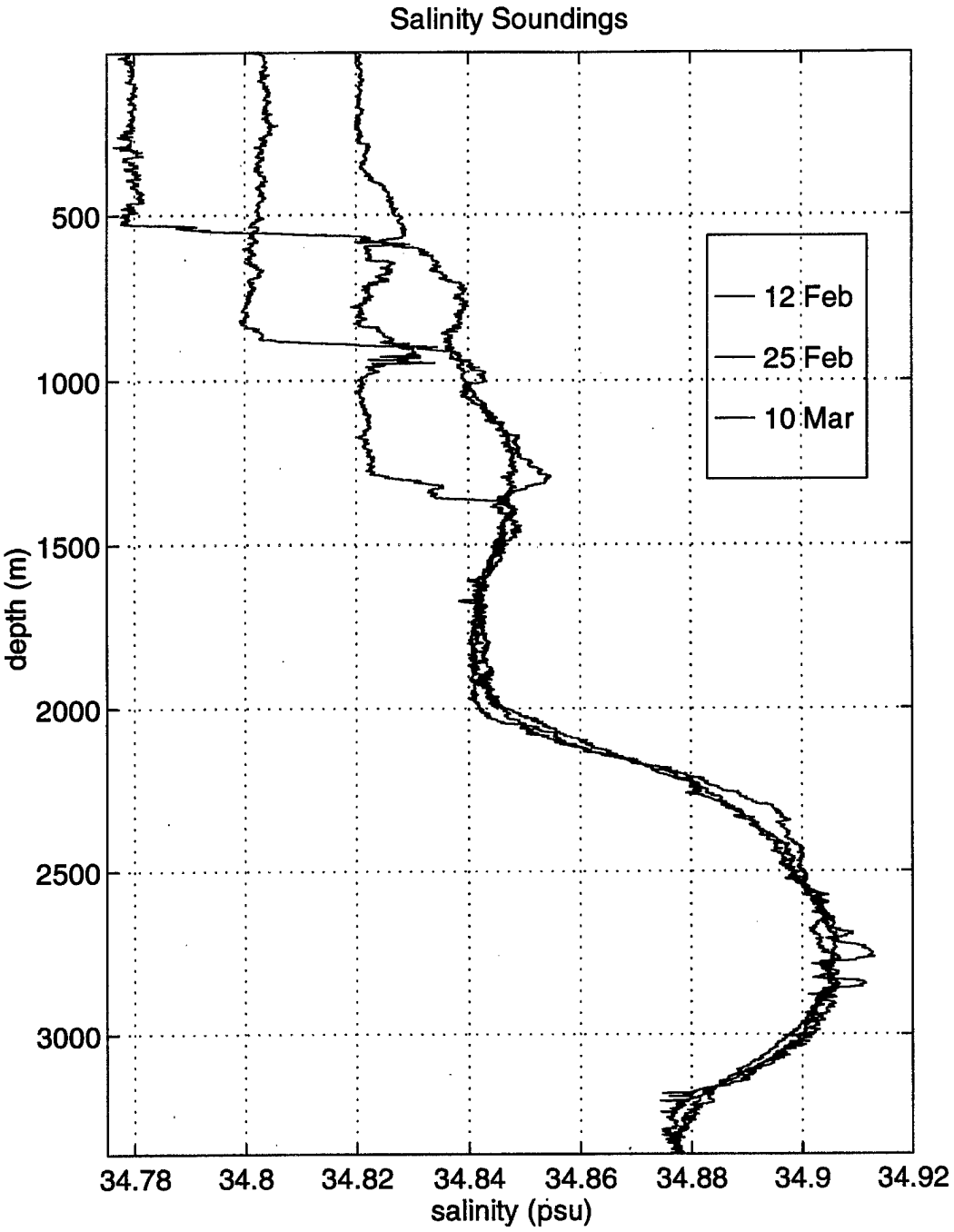

Figure 3.2: Observed salinity soundings for February 12, February 25 and March 10, 1997 at 57°N and 54°W. The 12 February profile has a least square fit correction applied. Note the mixed layer depth increased from 525 m, to 875 m, and finally to 1285 m, respectively.

IV. OBSERVATIONS

A. GENERAL ENVIRONMENTAL CONDITIONS

The Labrador Sea can present a harsh working environment especially during the winter. Throughout almost all of the 34 working days in the region (Fig 4.1), off-ice winds from the cold continental air mass predominated. During the experiment, February 7 to March 12, 1997, the mean air temperature was -8°C and the mean scalar wind speed was almost 12 m/s, and wind direction was usually between north and west. It was constantly cloudy and usually snowed, except for two sunny days. During the cruise, this precipitation of approximately 5 mm/day was observed almost every day contrary to a low number of forecasted events. Throughout this period, the net heat flux was often two standard deviations higher than normal because of the intense atmospheric conditions (Moore, personal communication).

Although air-sea interactions were observed over the entire period, model cases were only conducted over the 26 day period from February 12 (1639Z) to March 10 (1443Z) to coincide with the oceanographic data set available. For consistency, data presented and discussed is also limited to the same 26 day period.

1. Surface Fluxes and Momentum Stresses

Strong mean atmospheric forcing occurred during the period, and many parameters displayed high variability (Table 1). This variability can be seen in the surface wind speeds (Fig 4.2), the air and sea surface temperatures (Fig 4.3), the surface sensible heat flux and surface latent heat flux (Fig 4.4), and the atmospheric surface pressure (Fig 4.5) throughout the time frame. Most data were collected in an unstable atmosphere as sea surface temperatures were consistently greater than air temperatures (Fig 4.3). The average net surface fluxes for each period were about the same. The average values were 384 W/m^2 for the entire period of 12 February to 10 March, 403 W/m^2 from 12 February to 25 February and 365 W/m^2 from 25 February to 10 March. These high surface fluxes were matched by high momentum fluxes as the wind speed averaged about 12 m/s (Fig 4.2) during the period.

Table 1. 12 February to 10 March Surface Data.

PROPERTY	MEAN	MIN	MAX	STD DEVIATION
air temperature (°C)	-8.518	-17.109	-1.818	2.899
sea surface temperature (°C)	2.848	-1.468	5.721	0.9589
pressure (mb)	994.8	973.4	1013.3	9.5
relative humidity (%)	67.695	41.987	88.393	6.983
wind speed (m/s)	11.630	0.669	24.201	3.691
downward longwave radiation (W/m^2)	238.602	151.866	284.308	21.617
upward longwave radiation (W/m^2)	327.222	306.212	341.191	4.536
net longwave radiation (W/m^2)	88.621	43.725	174.019	20.801
downward shortwave radiation (W/m^2)	35.227	0.0	582.500	73.278
upward shortwave radiation (W/m^2)	3.522	0.0	58.250	7.328
net shortwave radiation (W/m^2)	-31.704	-524.250	6.089	65.950
overall net radiation (W/m^2)	56.909	-422.094	170.749	64.410
latent heat flux (W/m^2)	154.126	14.378	305.118	45.253
sensible heat flux (W/m^2)	172.930	12.737	361.250	69.222
wind stress ($dynes/cm^2$)	2.701	0.0130	12.393	1.707

Although quantities were variable throughout the cruise, latent and sensible heat flux were generally well correlated. Both sensible and latent heat fluxes had maximum values on approximately 12 and 22 February, and 4 March (day 43, 53, and 63). This was consistent with the relative wind speed maximum (Fig 4.2) and air temperature (Fig 4.3) and

pressure minimums (Fig 4.5) during the same time frame. NOGAPS analysis confirmed that each of these strong atmospheric events was influenced by either a low pressure system or strong troughing over the southern portion of Greenland or the southwestern portion of the Greenland Sea. The 0000Z 4 March (day 63) analysis verifies the presence of a low pressure system over Greenland and the southwestern Greenland Sea (Fig 4.6). The associated effects of this system were extremely high surface and momentum fluxes in the Labrador Sea as latent and sensible heat fluxes combined for a total of over 600 W/m^2 while the wind speed reached 20 m/s.

2. Power Spectral Density

Power spectral densities were computed for turbulent heat fluxes, radiative heat fluxes and total heat fluxes (Fig 4.7). Turbulent heat flux was calculated from latent and sensible heat fluxes. In this case, most energy was associated with the large scale synoptic regime and shorter scale storms occurring on a time scale of approximately 3 days or greater. Next, radiative heat flux was calculated from upward and downward shortwave and longwave radiation. In this case, peaks at 1 day and higher frequency harmonics represent the diurnal solar forcing. The energy peak greater than 3 days was still present but much smaller compared to the turbulent spectra indicating that synoptic forcing affects radiation. Finally, the total heat flux included all turbulent and radiative heat fluxes. This density spectrum had amplitude peaks coinciding with both the radiative and turbulent heat flux spectral densities. Most energy was associated with the large scale synoptic regime but smaller scale synoptic features are still significant. A large energy peak was associated with the daily solar variations. These density spectra reinforce the importance of large and small scale synoptic features and even more so the diurnal effect of the sun on surface heat flux variations.

B. OCEAN PROPERTIES: TEMPERATURE AND SALINITY

As first described in Chapter II, the CTD profiles do indicate the same water mass and properties below 1500 m throughout the experiment period (Fig 3.1 and Fig 3.2). Additionally, both temperature and salinity profiles show that during a previous winter, the winter of 1992-1993 (Guest, personal communication), deeper convection occurred which

caused the mixed layer to deepen to 2000 m. As previously discussed in Chapter III, the three CTD casts were far from the boundary currents in an area suspected to have deep convection (Fig 4.1).

The profiles show that convection did occur during this time frame as the ocean mixed layer deepened from 525 m, to 875 m and finally to 1285 m in only 26 days. Although the casts were conducted at the same location, analysis and comparison shows some distinctive differences in each mixed layer suggesting that this may not be exactly the simple one dimensional case assumed at the onset for model purposes.

Both temperature and salinity profiles did show some variability in the upper portion of the water column, the exact cause of which is unknown. It is hypothesized that these intrusions of water had been advected either horizontally and/or vertically into the region. If these intrusions were not horizontally advected into the region, vertical motion must have been taking place. However, Harcourt (personal communication) showed, using a large-eddy simulation (LES) model on the same case, that such intrusions can occur as water at the base of the mixed layer is entrained with that above; it rises vertically, thus leading to the mixed layer possessing water of different properties for at least a temporary period.

If the warmer saltier water was horizontally advected into the area, the region could not have been undergoing active mixing during the time the soundings were taken. Dissolved oxygen concentrations were highest in the respective mixed layers, with the highest overall concentrations found in the 25 February mixed layer (Fig 4.8). Because the atmosphere is the main source of dissolved oxygen, high concentrations in the mixed layers suggest active mixing with surface water must have occurred recently.

Looking at the CTD casts individually, the 10 February profile shows approximately uniform salinity in the mixed layer, whereas the temperature profile reveals remnants of warm water below that was probably eroded from the previous seasons' warmer temperatures. The 25 February profile shows a more homogeneous mixed layer as temperature and salinity appear to be rather well mixed throughout the layer. By 10 March, intrusions of both heat and salt are present throughout the mixed layer as the two profiles are similar in shape. In this case, there are fronts or horizontal gradients with small temperature

and salinity intrusions occurring at similar depths. If these are permanent intrusions, the temperature and salinity differences would serve to maintain the stability of the water column. On the other hand, it is in this region specifically that Harcourt (personal communication) believes turbulent vertical motion caused these temporary changes to the mixed layer. Although these differences in temperature and salinity are present, they are nearly compensating deviations such that the mixed layer density is almost constant, therefore allowing the original supposition of a one dimensional case and use of the one dimensional model.

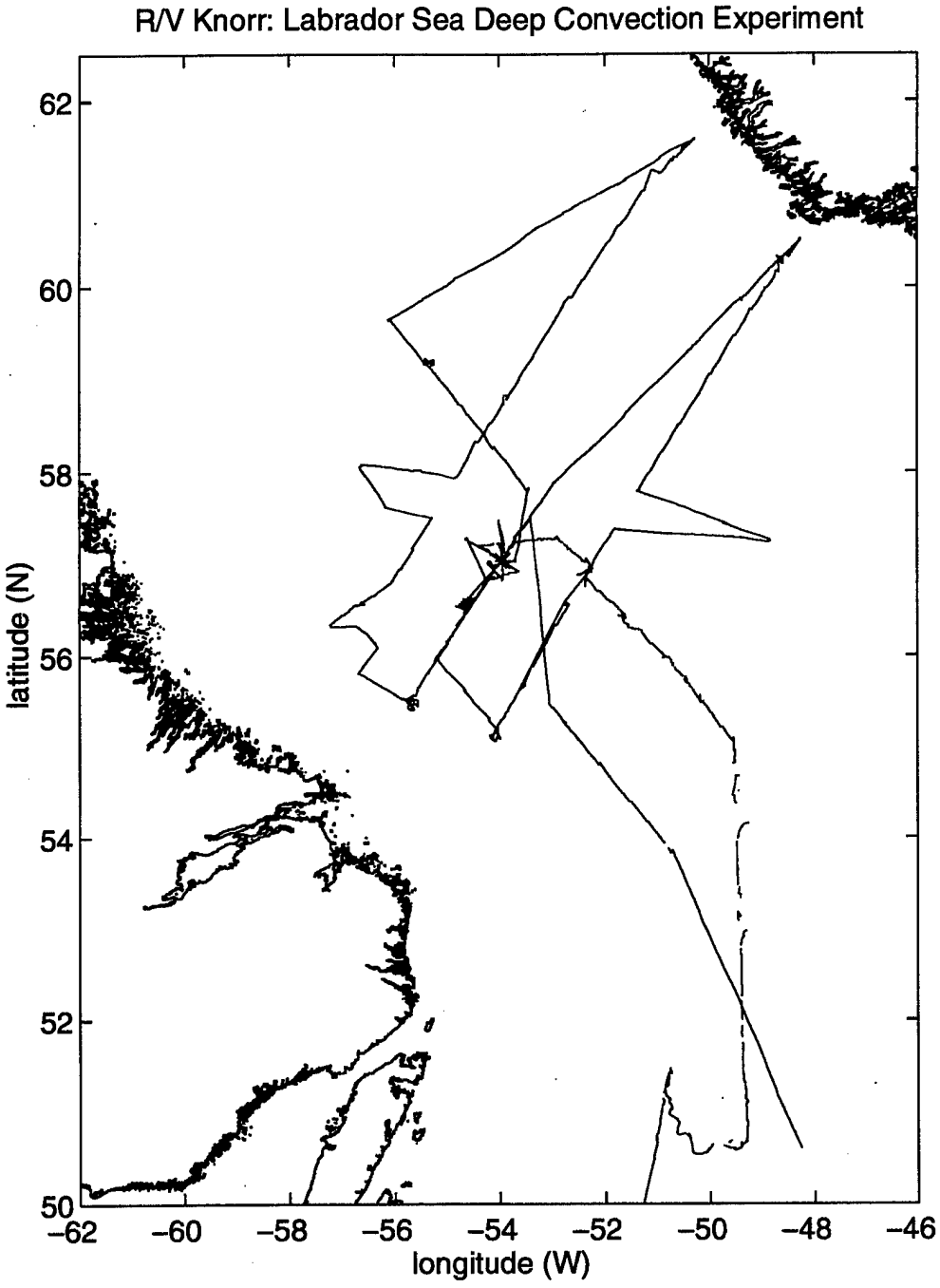

Figure 4.1: The R/V Knorr's cruise path in the Labrador Sea during the Labrador Sea Deep Convection Experiment during the winter of 1997. The red '*' in the center represents the February 12, February 25 and March 10 CTD locations.

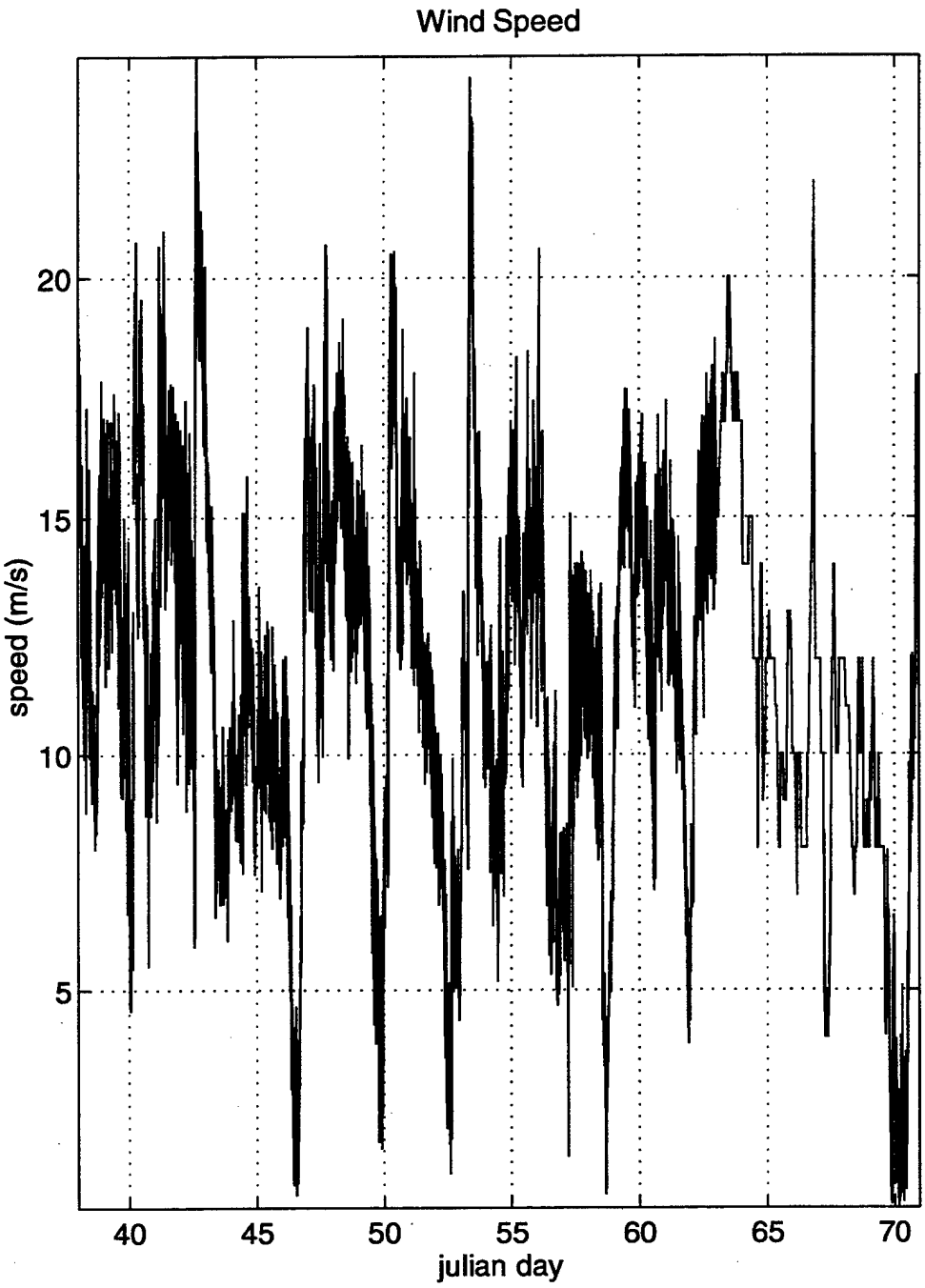

Figure 4.2: Time series of wind speed (m/s) data in the Labrador Sea during the winter of 1997. Wind speeds were highly variable throughout the period.

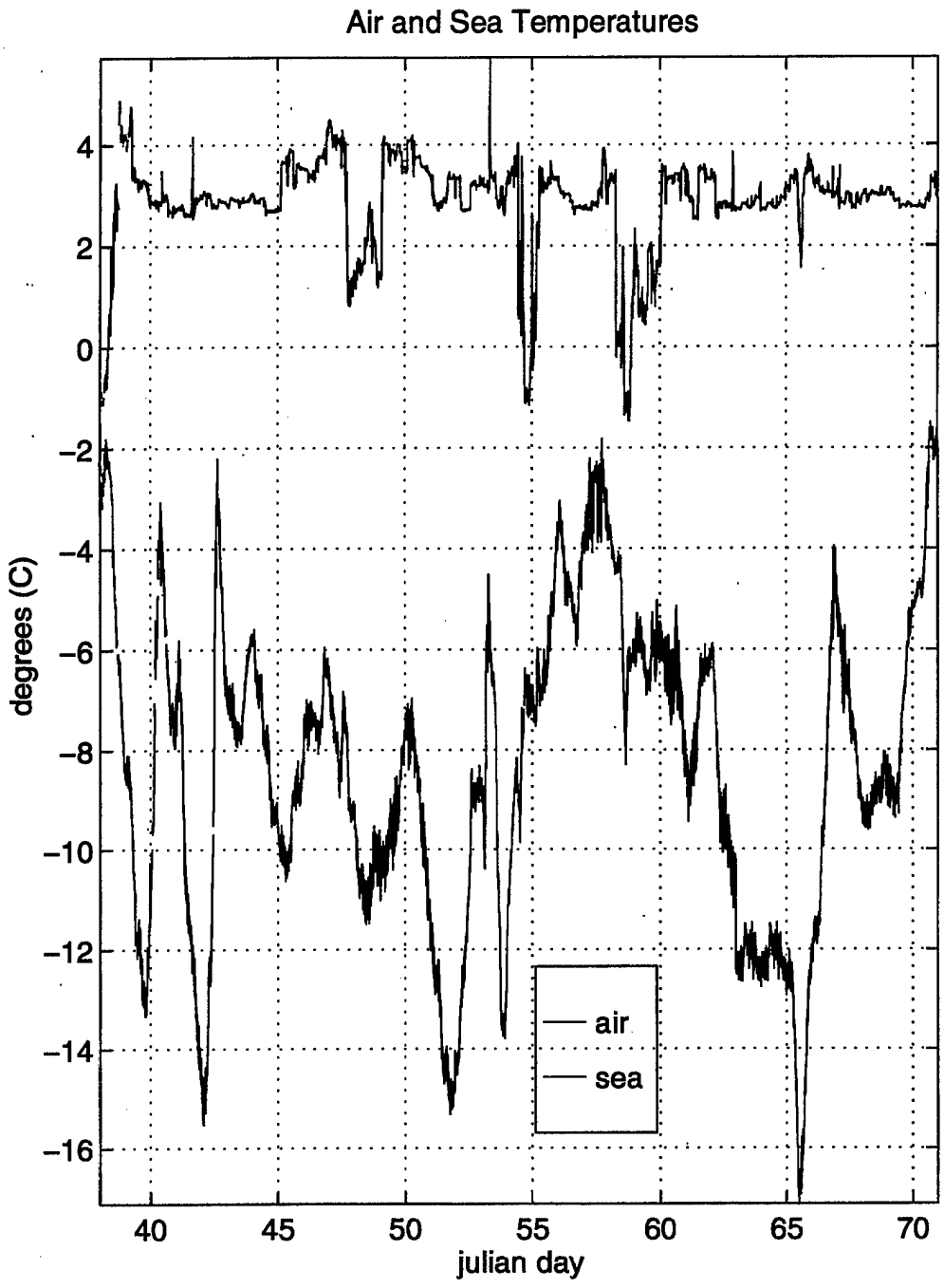

Figure 4.3: Time series of air and sea surface temperatures (°C) in the Labrador Sea during the winter of 1997. Air temperature was highly variable throughout the period and there was consistently a large air-sea temperature difference.

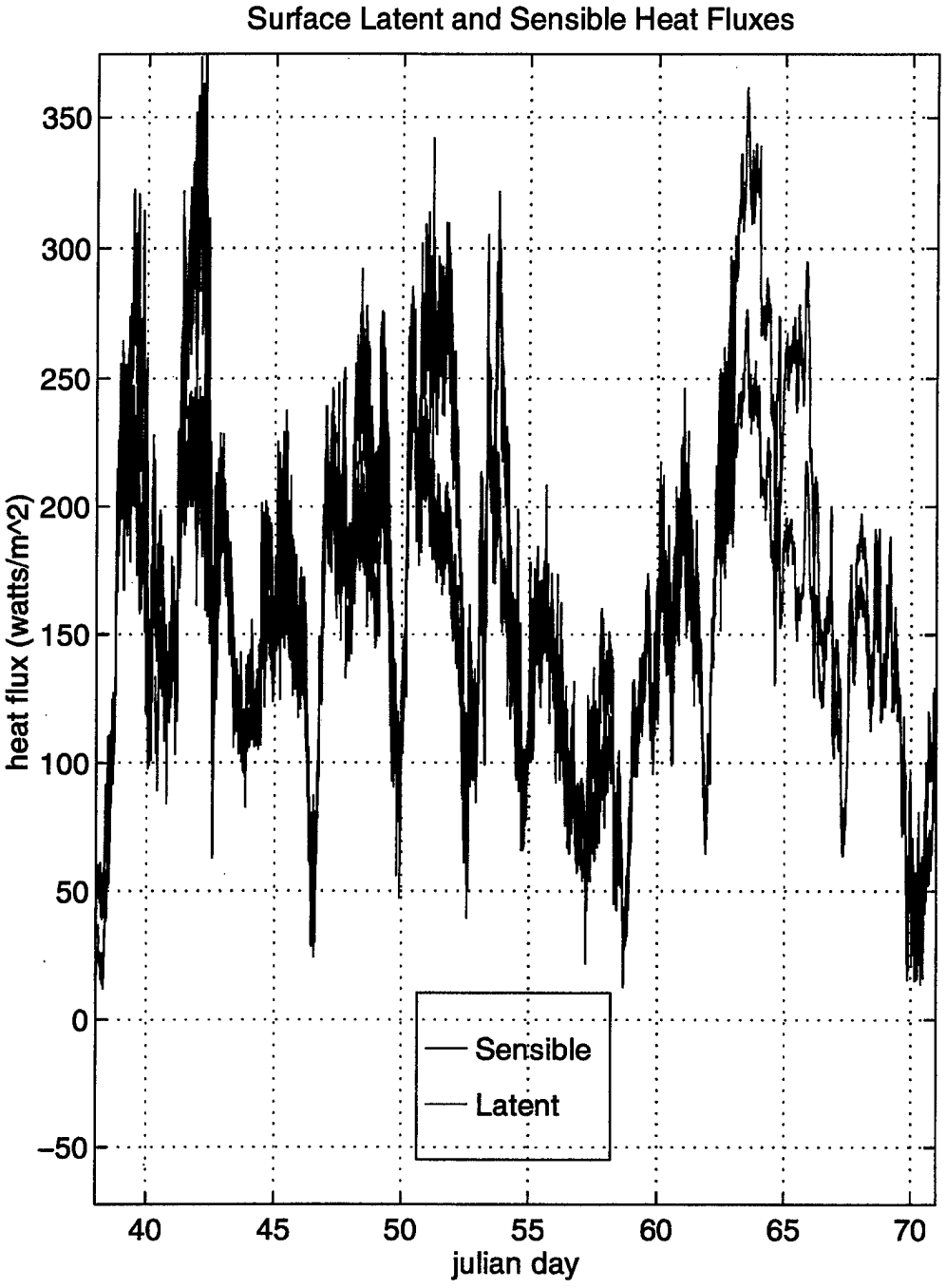

Figure 4.4: Time series of surface latent and sensible heat flux (watts/m^2) in the Labrador Sea during the winter of 1997. Both show the effects of strong forcing and high variability throughout the period.

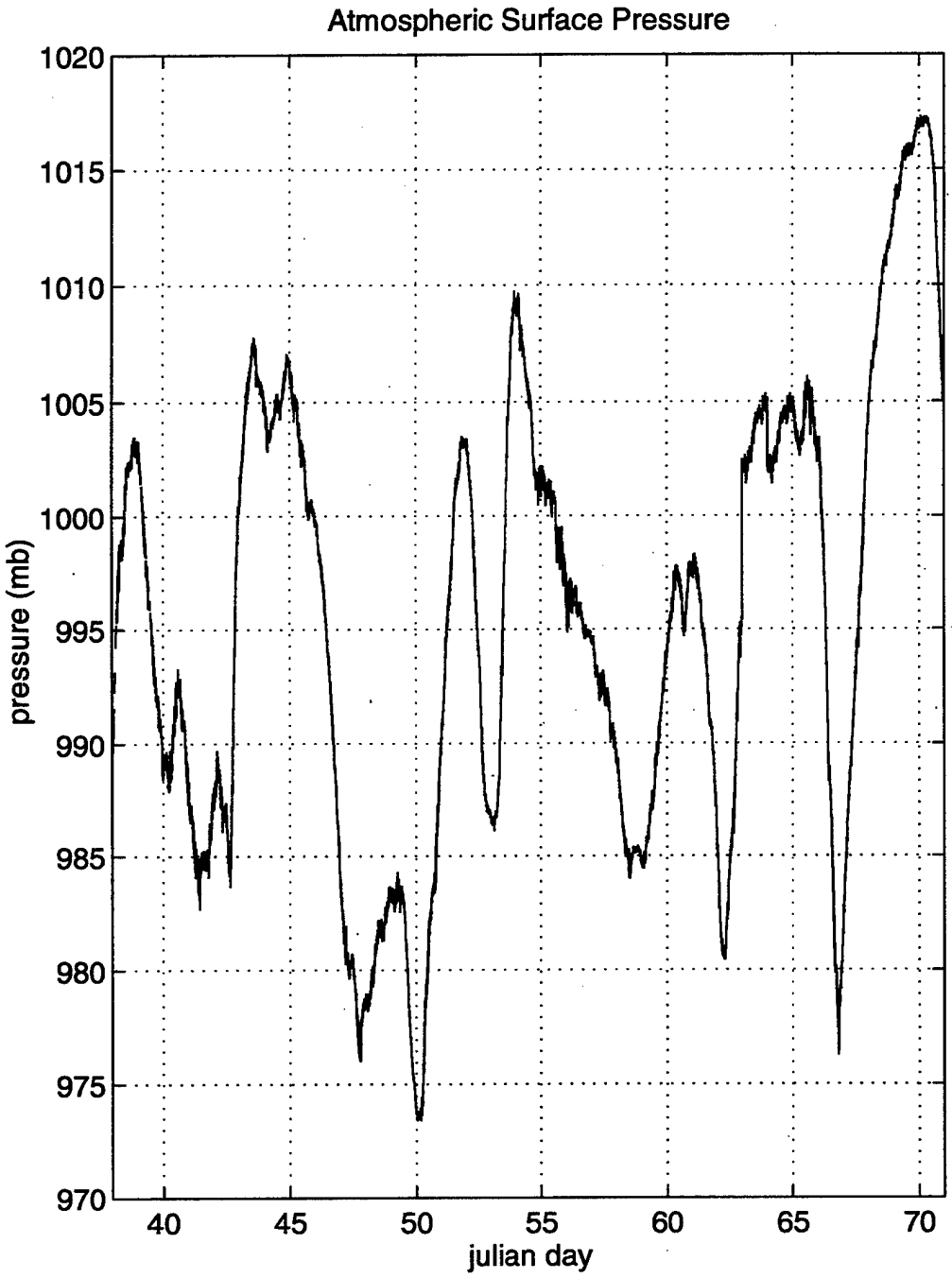

Figure 4.5: Time series of atmospheric surface pressure (mb) in the Labrador Sea during the winter of 1997. Pressure was variable throughout the period.

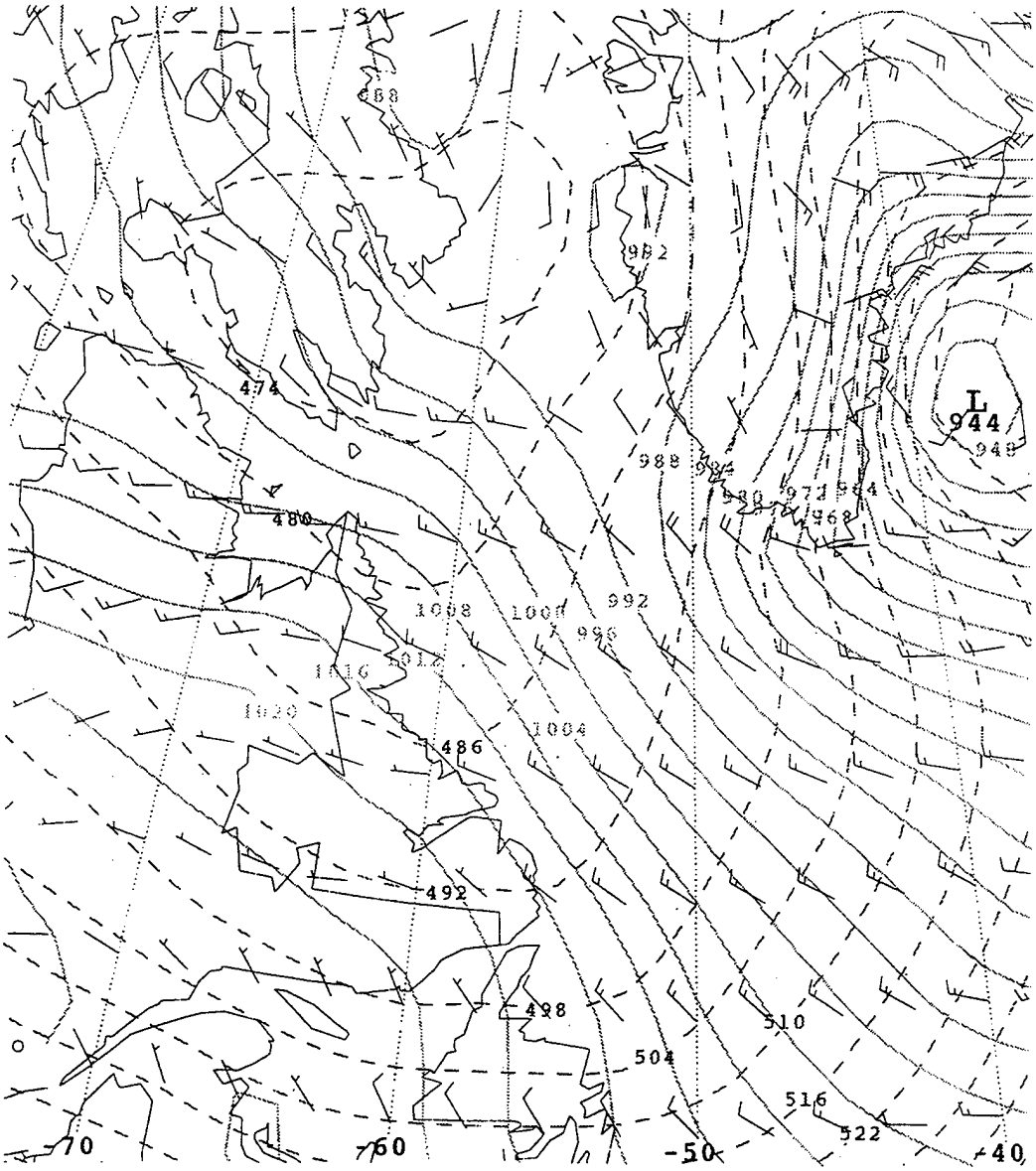

Figure 4.6: NOGAPS 0000Z 4 March 1997 analysis of mean sea level pressure and 1000 - 500 mb thickness. The low pressure system just east of Southern Greenland led to strong atmospheric forcing with extremely high surface and momentum fluxes in the central Labrador Sea.

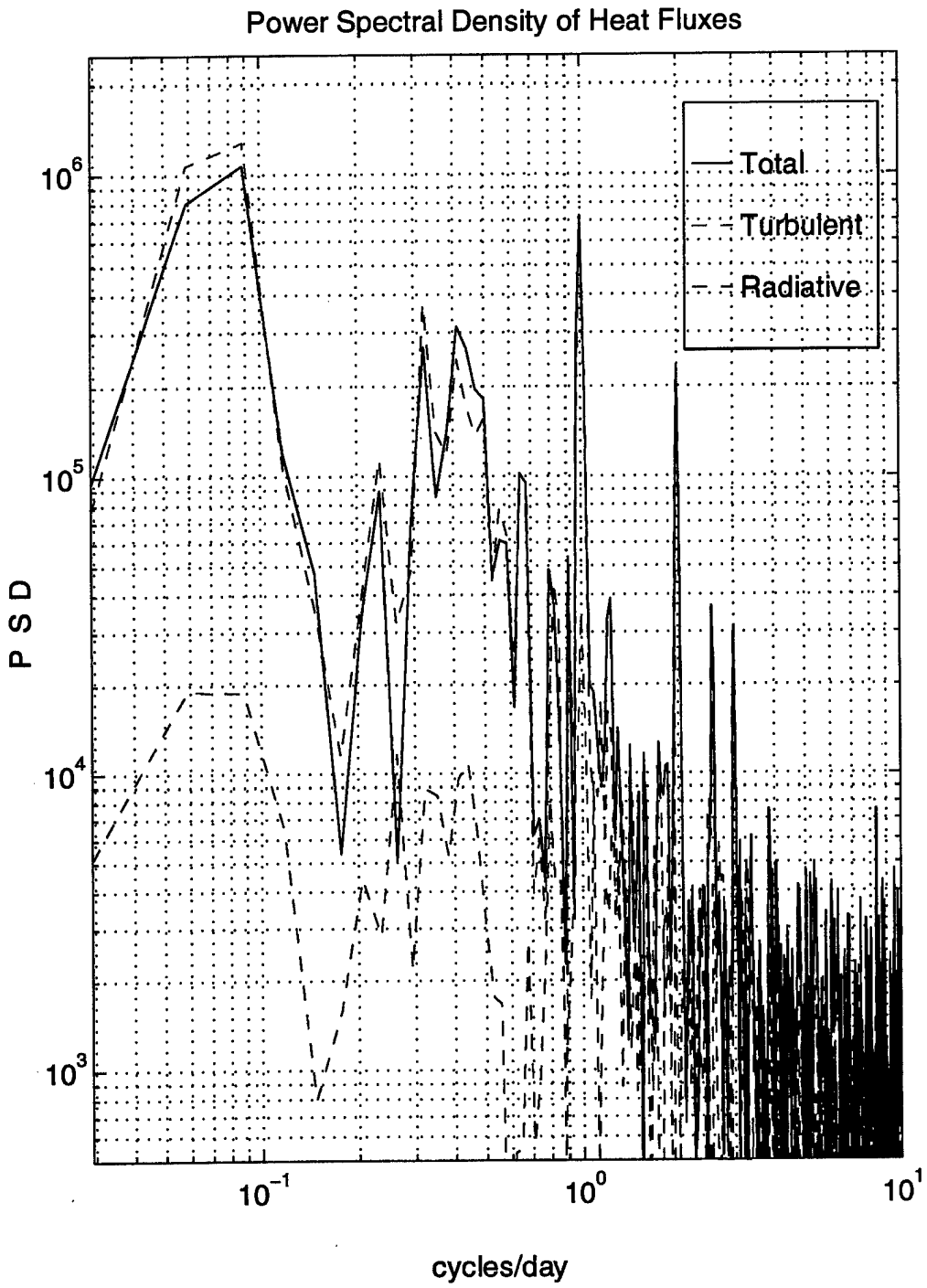

Figure 4.7: Power spectral densities (cycles/day) of total, turbulent and radiative heat fluxes. Energy peaks occurred at 10, 3, 1 and ½ days which represent long and short term synoptic scale storm systems, daily and diurnal solar variations, respectively.

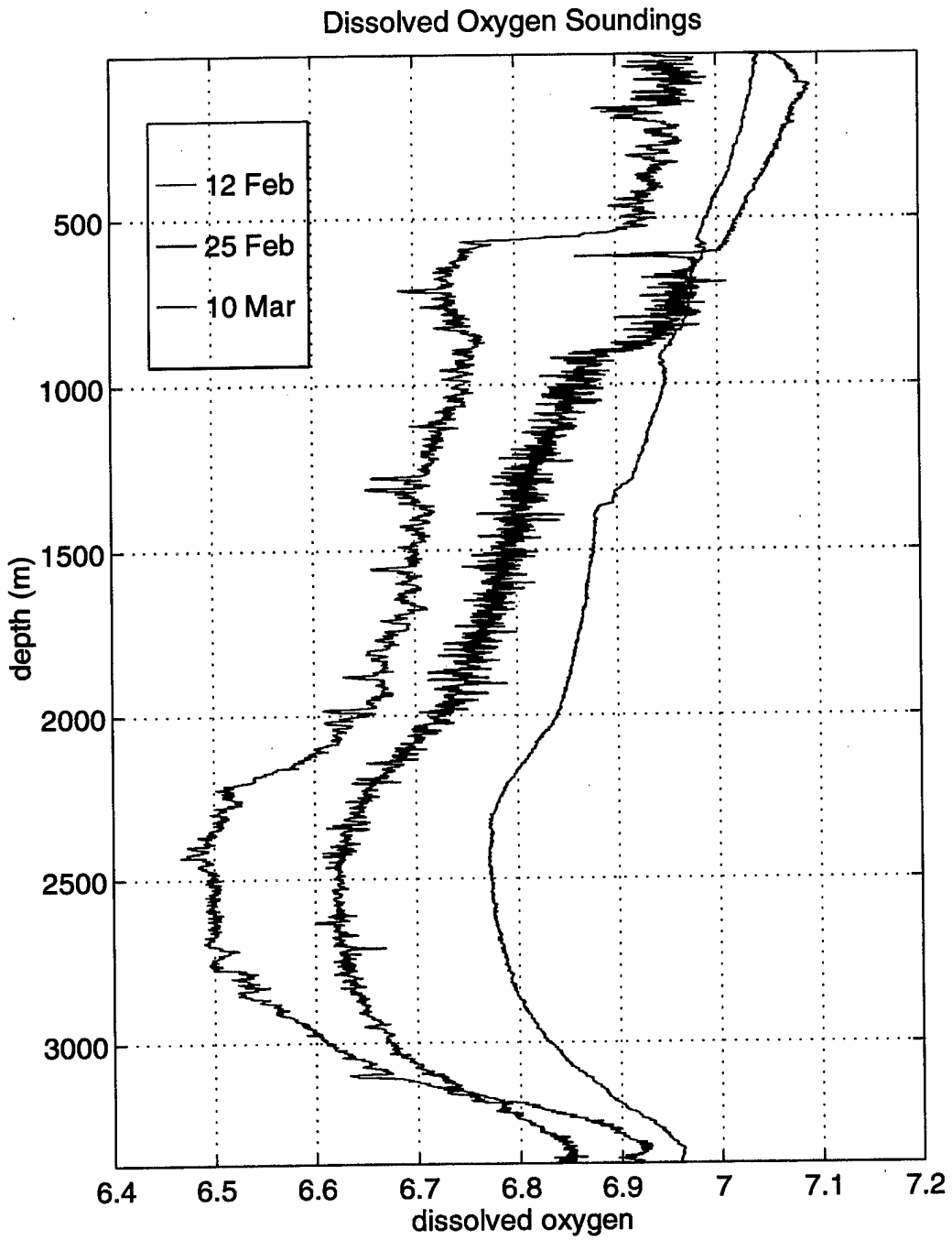

Figure 4.8: Observed dissolved oxygen soundings (μmol/kg) for February 12, February 25 and March 10, 1997 at 57°N and 54°W.

V. EXPERIMENTS

A. TEMPERATURE AND SALINITY

In an idealized one dimensional ocean-atmosphere system, the integrated ocean heat loss would equal the atmospherically forced surface fluxes and model predictions of mixed layer temperature, salinity and depth would be exactly consistent with measured CTD profiles. Although this was not such a perfect system, comparisons of ocean heat and salt loss with measured fluxes give some insight to conditions occurring in the Labrador Sea. The three CTD profiles of temperature and salinity were utilized in order to determine the integrated heat and salt loss of the Labrador Sea between the casts and over the entire period from 12 February to 10 March.

1. Ocean Heat Loss

The integrated ocean heat loss was determined by calculating the total heat at each level:

$$Q=\rho c_p z \Delta T \tag{5.1}$$

dividing by the time difference between each sounding and summing the values leads to the heat loss, transformed into a net heat flux. Calculations were only performed from the surface to 1500 m as the profiles showed little change in temperature or salinity below 1500 m.

The measured ocean heat loss and observed atmospheric fluxes were comparable over the entire period but showed significant variability during the individual periods probably due to atmospheric mesoscale effects (Table 2). The magnitude of the ocean heat loss calculated for the first 13 days was 57% greater than the net atmospheric heat flux. The large amount of heat associated with the warm water below the mixed layer had to be removed in order to achieve the uniform 25 February mixed layer temperature profile. On the other hand, the integrated heat loss associated with the next 13 days was 42% less than the atmospheric fluxes. Overall, comparison of the measured ocean heat loss and the observed atmospheric fluxes for the entire period led to much more consistent values (within 11.5%).

Table 2. Integrated Ocean Heat Loss Compared with Measured Heat Flux Values (Sensible Heat Flux + Latent Heat Flux + Net Radiation).

PERIOD	MEASURED OCEAN HEAT LOSS	ATMOSPHERIC HEAT FLUXES
12 February - 25 February	633 W/m^2	403 W/m^2
25 February - 10 March	212 W/m^2	365 W/m^2
12 February - 10 March	428 W/m^2	384 W/m^2

There are several possible reasons for the differences between the integrated ocean heat loss and the observed surface fluxes. Differences in the measured atmospheric fluxes from 25 February to 10 March suggest that a patch of cold, fresh water could have been horizontally advected into the region. Errors could have been introduced from the instrumentation or from the bulk parameterization calculations. Finally, variations could have been caused by the CTD location not being coincident with the location of the ship where the fluxes were measured. Because the ship moved throughout the Labrador Sea between CTD casts, conditions at these locations could have been significantly different from what was occurring at the CTD station. Any or all of these reasons could have contributed to the significant difference between calculated and observed heat fluxes.

2. Ocean Salt Loss

Evaporation of seawater increases its salinity by increasing the concentration of salt in the water. A total salt loss was calculated for the period using the salinity profiles and converting it to an equivalent latent heat flux. Assuming zero precipitation, the salt loss was calculated by measuring the change in salinity at each level:

$$Q_E = \frac{\rho L z \Delta S}{S} \tag{5.2}$$

Dividing by the time difference between each sounding and summing the values yields an equivalent latent heat flux. Values were only calculated to 1500 m, as corrected salinity profiles were almost unchanged below 1500 m.

The equivalent latent heat flux also varied significantly from the measured latent heat flux during the periods (Table 3). During the first 13 days, the equivalent latent heat flux was 26% smaller than the measured latent heat flux. On the other hand, the equivalent latent heat flux associated with the next 13 days was 270% greater than the measured flux which showed little variability. This led to an overall equivalent latent heat flux 115% greater than the measured latent heat fluxes over the entire period.

Table 3. Integrated Ocean Salt Loss (converted to Equivalent Latent Heat Flux) Compared with Measured Latent Heat Flux Values.

PERIOD	EQUIVALENT LATENT HEAT FLUX	MEASURED LATENT HEAT FLUX
12 February - 25 February	116 W/m^2	157 W/m^2
25 February - 10 March	559 W/m^2	151 W/m^2
12 February - 10 March	332 W/m^2	154 W/m^2

Equivalent latent heat flux should be slightly less than the measured fluxes due to the assumption of no precipitation. Variations could be due to horizontal and/or vertical advection of an 'unspicy' patch of cold, fresh water after the 25 February profile. If there was ice formation, brine rejection could have introduced more salinity into the region than could be described by the measured fluxes. Lastly, it is possible that the CTD casts sampled an entirely different water mass that was present in the surface layer. Any one (or any combination) of these reasons could have led to the difference between the measured and calculated surface flux variations.

Unlike the integrated ocean heat loss, equivalent and observed latent heat fluxes were significantly different at the end of the period. Overall the salinity and temperature changes caused the density to increase slightly throughout the period.

B. MODEL INTEGRATIONS

Experimental model integrations were conducted utilizing the NPS one dimensional model and data collected during the Labrador Sea Deep Convection Experiment. The model was initialized with the 12 February temperature and salinity profiles (Fig 5.1). Various

model integrations were conducted for the 26 day period (days 43 through 69) forcing the model with atmospheric data from shipboard observations which included wind stress (associated wind speed is described in Fig 4.2), sensible and latent heat fluxes (Fig 4.4), net radiation, and downward shortwave radiation.

After completion of the model integrations, comparisons between the 25 February and 10 March observed profiles of temperature and salinity with the same model predicted data were analyzed to verify changes to the mixed layer temperature, salinity and depth both spatially and temporally. Finally, hypothetical model integrations were conducted in order to quantify the types and strength of atmospheric forcing which could cause the present and deepened (2000 m) mixing. Other than the first set of averaging interval variations, all subsequent model integrations were initialized with the baseline data and included only the variations so specified.

The observed mixed layer deepened from 525 m to 875 m and finally to 1285 m during the 26 day period. The model integrations were conducted to not only verify this deepening but also deeper convection to 2000 m.

1. Baseline Case: Model vs Observations

The first model integration was conducted to establish a baseline case. This case had the highest resolution of data, was considered most accurate and thus was used as the basis of comparison for all other model integrations. All heat fluxes and wind stresses were averaged hourly over the entire period. Precipitation minus evaporation was set equal to zero as both values were offsetting, based on initial precipitation estimates. The 12 February salinity profile was corrected with the linear least square fit as described in Chapter III.

The baseline case led to a model predicted mixed layer depth of 1361 m (Fig 5.2) and the model profiles matched observations of temperature well within measurement uncertainty. Although model predicted mixed layer potential temperatures and salinity values were different than those observed, model and observed mixed layer potential density values were very consistent (Fig 5.3).

2. Averaging Interval Variations: Fluctuating vs Constant Forcing

Five separate model integrations were conducted to compare the baseline case of hourly averaged data with the hourly data points (from 5 minute averaged data), data averaged over a day (24 hour period), data averaged over a week (7 day period) and finally constant forcing over the entire period (12 February to 10 March). For these cases, the only change imposed was the averaging interval of the input heat fluxes and wind stresses (Fig 5.4). These model integrations were compared (Table 4) to determine if they caused differences in mixed layer temperature or salinity (Fig 5.5) and mixed layer depth (Fig 5.6).

Storms can affect atmospheric forcing for a period of hours to days and cause relative maxima in wind stress and surface fluxes (Fig 5.4). The case with constant forcing over the entire period was expected to cause a shallower mixed layer depth since storms and other individual events would be averaged and thus felt less intensely; this did occur, but the differences were small. Some variations in the mixed layer temperatures (weaker deepening) were evident due to the averaging of the strong fluxes and wind stresses around days 47, 54 and 66 (Fig 5.5).

Table 4. Averaging Interval Variations and Associated Model Predicted Mixed Layer Depths.

VARIABLE	MIXED LAYER DEPTH (m)
OBSERVED	1285
hourly averaged data (BASELINE)	1361
hourly data	1367
daily averaged data	1359
weekly averaged data	1349
entire period averaged (12 Feb - 10 Mar)	1347

These different model integrations showed little variability in the final values. In all cases, the mixed layer temperatures initially increase due to the mixing of intermediate

warmer water with the colder surface water. After approximately five days, mixed layer temperatures decrease for the rest of the period. The mixed layer salinity values steadily increase as more saline water is entrained into the mixed layer.

A comparison of model output profiles for 25 February shows that predicted mixed layer temperatures are approximately 0.75°C warmer than the observed temperatures, while model salinity values were only slightly greater than those observed (Fig 5.7). Although temperature and salinity values were not exactly verified, observed and predicted mixed layer depths differed by only 76 m or within 6%. The 10 March profile showed much better agreement with the predicted temperature. Here the model accurately portrayed the mixed layer temperature while predicted salinity values were slightly lower than observed.

These model solutions showed that the fluctuating forcing cases did cause slightly more deepening, but the most important factor was the overall mean influence of the surface fluxes. The major cause of mixed layer deepening appears to be the total amount of heat lost over the period; therefore, in these cases with only small changes due to the averaging technique, the mixed layer depth did not change significantly among the separate model integrations.

3. Surface Flux and Radiation Variations

Next, a number of model integrations were conducted varying the surface sensible heat fluxes, latent heat fluxes, solar and net radiations to attempt to quantify their effects and observe the sensitivity of mixed layer depth to changes. Cases were conducted both increasing and decreasing these values to see the magnitude of the effects (Table 5).

Such changes included decreasing the net fluxes (net radiation, latent and sensible heat flux) by 50%, increasing the fluxes by 50% and finally increasing the fluxes by 100% (Fig 5.8). For each of these cases, mixed layer temperature slightly increases over the first few days, then decreases over the rest of the period. The length of time the temperature increases is shortest for the largest fluxes and longest for the smallest fluxes. In addition, the smaller the heat flux, the smaller the overall temperature change. Mixed layer salinity increased throughout the entire period with the smallest overall change associated with the

lowest heat flux. As expected, increases to the surface fluxes and net radiation values caused a deepening of the mixed layer whereas decreases resulted in a shallower mixed layer (Fig 5.8).

Table 5. Surface Flux and Radiation Variations and Associated Model Predicted Mixed Layer Depths.

VARIABLE	PERCENT CHANGE	MIXED LAYER DEPTH (m)
OBSERVED	0 %	1285
BASELINE	0 %	1361
latent heat flux	(-) 50%	1217
sensible heat flux	(-) 50%	1202
latent + sensible heat flux	(-) 50%	1073
net radiation	(-) 50%	1305
latent + sensible heat + net radiation	(-) 50%	1026
latent heat flux	(-) 30%	1271
sensible heat flux	(-) 30%	1261
latent + sensible heat flux	(-) 30%	1181
net radiation	(-) 30%	1326
latent + sensible heat +net radiation	(-) 30%	1152
solar radiation	(-) 30%	1379
latent heat flux	(+) 30%	1454
sensible heat flux	(+) 30%	1465
latent + sensible heat flux	(+) 30%	1564
net radiation	(+) 30%	1396
latent + sensible heat + net radiation	(+) 30%	1604
solar radiation	(+) 30%	1344

Table 5. Continued.

VARIABLE	PERCENT CHANGE	MIXED LAYER DEPTH (m)
OBSERVED	0 %	1285
BASELINE	0 %	1361
latent heat flux	(+) 50%	1519
sensible heat flux	(+) 50%	1540
latent + sensible heat flux	(+) 50%	1718
net radiation	(+) 50%	1418
latent + sensible heat + net radiation	(+) 50%	1787
solar radiation	(+) 50%	1333
latent heat flux	(+)100%	1696
sensible heat flux	(+)100%	1740
latent + sensible heat flux	(+)100%	2124
net radiation	(+)100%	1476
latent + sensible heat + net radiation	(+)100%	2227

Model predicted mixed layer profiles were also compared to the final observed profiles of temperature and salinity (Fig 5.9). Model temperatures were colder than the observed temperatures for increases in the surface fluxes since increasing the surface fluxes would cause more heat to be transferred resulting in colder temperatures. On the other hand, increases in surface fluxes caused model mixed layer salinity values to be greater than the observed salinities while decreases in the fluxes had the opposite effect. Because the average latent heat flux was less than the average sensible heat flux, a similar percentage change in each resulted in sensible heat flux having a larger impact on the mixed layer depth. By comparison, an increase of sensible, latent and net radiation caused a larger depth increase than the same percentage decrease of latent, sensible and radiative caused shallowing.

4. Wind Stress Variations

This set of model integrations consisted of variations of the wind stress to measure the effect on the mixed layer depth. Although both wind stress and buoyancy can cause mixing, wind stress alone did not have a large effect on the mixed layer depth (Table 6). Periods of high wind stress did show the most intense deepening and these gradients were consistent in the separate model integrations (Fig 5.10). Comparing the wind stress and surface heat fluxes, similar percentage changes of the heat fluxes caused much greater changes to the mixed layer depth. Although wind stress provides TKE to the mixed layer, it alone does not appear to have as significant effects on mixed layer temperature, salinity and depth as other parameters.

Table 6. Wind Stress Variations and Associated Model Predicted Mixed Layer Depths.

WIND STRESS PERCENT CHANGE	MIXED LAYER DEPTH (m)
OBSERVED	1285
(-) 50%	1319
(-) 30%	1334
0 % (BASELINE)	1361
(+) 30%	1391
(+) 50%	1411
(+) 100%	1465

5. Precipitation Variations

In this group of model integrations, precipitation was introduced to observe its effect on the mixed layer depth. Because observed salinity was actually greater than the model salinity, from the onset this group of model predictions including precipitation should cause the mixed layer depth to be too shallow. It snowed constantly during the cruise and rough estimates of snowfall (5 cm/day) showed that precipitation was approximately equal to the evaporation. No evaporative salinity flux was introduced into the model, so the effects of

the precipitation could be specified (Table 7). These mixed layer depths show that zero or 5 mm/day precipitation was consistent with the mixed layer depth data and observations. Even though measurements of precipitation were not precise, the model predictions imply that 10 mm/day of precipitation shoals the mixed layer too much and therefore could not be consistent with the actual conditions unless there was salt input from other sources such as more latent heat flux, brine rejection or advection.

Model predicted mixed layer profiles were also compared to the final 10 March observed profiles of temperature and salinity (Fig 5.11). As the amount of precipitation was increased, the mixed layer cools more and deepens less. Also as precipitation was increased, the mixed layer salinities decreased significantly. Although 5 mm/day of precipitation seems to accurately predict the mixed layer temperature and depth, salinity values were almost 0.02 psu lower than those observed.

Table 7. Precipitation Variations and Associated Model Predicted Mixed Layer Depths.

PRECIPITATION AMOUNT	MIXED LAYER DEPTH (m)	10 MAR: MIXED LAYER SALINITY(psu)
OBSERVED	1285	34.823
0 mm/day (BASELINE)	1361	34.817
5 mm/day	1253	34.811
10 mm/day	1152	34.808

6. Mixed Layer Salinity Variations

These model integrations were conducted to observe the sensitivity to changes in the initial mixed layer salinity (Fig 5.12). This simulates salinity advection in the mixed layer for these cases. The 12 February mixed layer salinity was offset either positively or negatively by the amount specified (Table 8).

Model predicted mixed layer profiles were also compared to the 25 February and 10 March salinity profiles (Fig 5.13). Although a model salinity offset of (-) 0.01 psu resulted in a mixed layer depth comparable to the 25 February observed mixed layer depth, salinities

were much lower than those observed. The same model solution resulted in even a larger discrepancy between the model and observed mixed layer salinity of 10 March. In actuality, all salinity offset profiles resulted in model mixed layer salinities that were more different from observations than the baseline case. Although the (-) 0.01 psu salinity offset gave a reasonable mixed layer depth, other properties were so far off that this case could not be considered reasonable.

Table 8. Initial Mixed Layer Salinity Variations and Associated Model Predicted Mixed Layer Depths.

MIXED LAYER SALINITY OFFSET (psu)	MIXED LAYER DEPTH (m)	25 FEB MIXED LAYER SALINITY (psu)	10 MAR MIXED LAYER SALINITY (psu)
(-) 0.02	1118	34.789	34.807
(-) 0.01	1234	34.796	34.811
OBSERVED	1285	34.804	34.823
0 (BASELINE)	1361	34.806	34.817
(+) 0.01	1493	34.814	34.823
(+) 0.02	1632	34.821	34.828

7. Surface Flux and Wind Stress Variations: Possible Mixing to 2000 m

A first analysis of the CTD profiles led to the question concerning what it would take to mix down to the maximum depth achieved several years ago. The observed temperature and salinity profiles (Fig 3.1 and Fig 3.2) both show deepened convection occurred down to 2000 m previously as indicated by the increase in salinity and increase/decrease in temperature. These model integrations were conducted to attempt to deepen the mixed layer to 2000 m (Table 9). For this experiment, the surface fluxes and wind stresses were changed to try to deepen the mixed layer. For some less than extreme atmospheric conditions, the mixed layer depth could very easily be deepened to 2000 m. In all cases, similar changes in

the heat flux variations had a larger effect on the mixed layer depth than wind stress variations. These variations show the likelihood of enhanced mixed layer deepening in the Labrador Sea to at least 2000 m.

Table 9. Surface Flux and Momentum Stress Variations and Associated Model Predicted Mixed Layer Depths.

VARIABLE	PERCENT CHANGE	MIXED LAYER DEPTH (m)
OBSERVED	0 %	1285
latent heat flux sensible heat flux wind stress	(+) 75% (+) 75% (+) 30%	1947
latent heat flux sensible heat flux net radiation	(+) 75% (+) 75% (+) 75%	2034
latent heat flux sensible heat flux wind stress	(+) 100% (+) 100% (+) 30%	2136
latent heat flux sensible heat flux net radiation wind stress	(+) 100% (+) 100% (+) 100% (+) 100%	2259

8. Storm Variations (Wind Stress Variations)

How much of a difference individual storms make and whether they are more effective at certain times is not known. In these model integrations, an individual storm was added to the baseline case with the only variability consisting of wind stress variations (Fig 5.14). The mean wind stress of the entire period was preserved such that as the storm strength increased, the overall forcing for the rest of the period was decreased. This maintained constant wind stress over the entire period (in comparison to the baseline case) and allowed the isolation of the storm itself. In all cases, a significant increase in the momentum stress was needed to show any notable variability between the storms. The five

day storm was included at the beginning (day 44 - 48), middle (day 53 - 57) and end (day 63 - 67) of the period to see the effect on the mixed layer depth (Table 10).

Table 10. Five Day Storm Variations and Associated Model Predicted Mixed Layer Depths.

WIND STRESS CHANGE	STORM PERIOD Julian days	MIXED LAYER DEPTH (m)
OBSERVED	N/A	1285
BASELINE	N/A	1361
$u_*^2 * 2$ (+ 100%)	44-48 53-57 63-67	1350 1354 1360
$u_*^2 * 3$ (+ 200%)	44-48 53-57 63-67	1343 1349 1359
$u_*^2 * 4$ (+ 300%)	44-48 53-57 63-67	1338 1345 1358
$u_*^2 * 5$ (+ 400%)	44-48 53-57 63-67	1334 1342 1356
$u_*^2 * 6$ (+ 500%)	44-48 53-57 63-67	1331 1340 1354
$u_*^2 * 7$ (+ 600%)	44-48 53-57 63-67	1329 1338 1353
$u_*^2 * 8$ (+ 700%)	44-48 53-57 63-67	1327 1336 1351

Each of the model integrations showed the same characteristics; the storm at the end of the period was slightly more effective resulting in the deepest predicted mixed layer depth (Fig 5.15). This can be described mathematically by looking at an approximation to the mixed layer depth equation (Garwood, 1977):

$$\frac{\partial h}{\partial t} = \frac{\frac{u_*^3}{h} + \alpha g \frac{Q_o}{\rho c_p}}{\alpha g \Delta T - \beta g \Delta S} \tag{5.3}$$

First this shows that the friction velocity cubed is directly related to deepening rate. The higher the wind stress driven turbulence, the more mixing that occurs for a smaller depth per unit volume. Once the mixed layer has significantly deepened, as in the first cases where u_*^2 is increased by 200% and 300%, wind stress will have less of an effect on deepening. This effect can also be described by considering the buoyancy jump. As the mixed layer deepens, there is a smaller buoyancy jump across the bottom of the mixed layer; therefore, for the same u_*, the mixed layer depth will increase as buoyancy jump is decreased.

Both of these possibilities can explain why there is less variability between the predicted mixed layer depths for the late period storms compared with the storms at the beginning of the period. The stronger storms at the end are able to deepen the mixed layer almost as deep even though there was significantly weaker forcing throughout the rest of the period. Overall constant wind stress was more effective at mixing than variable wind stress for the same mean.

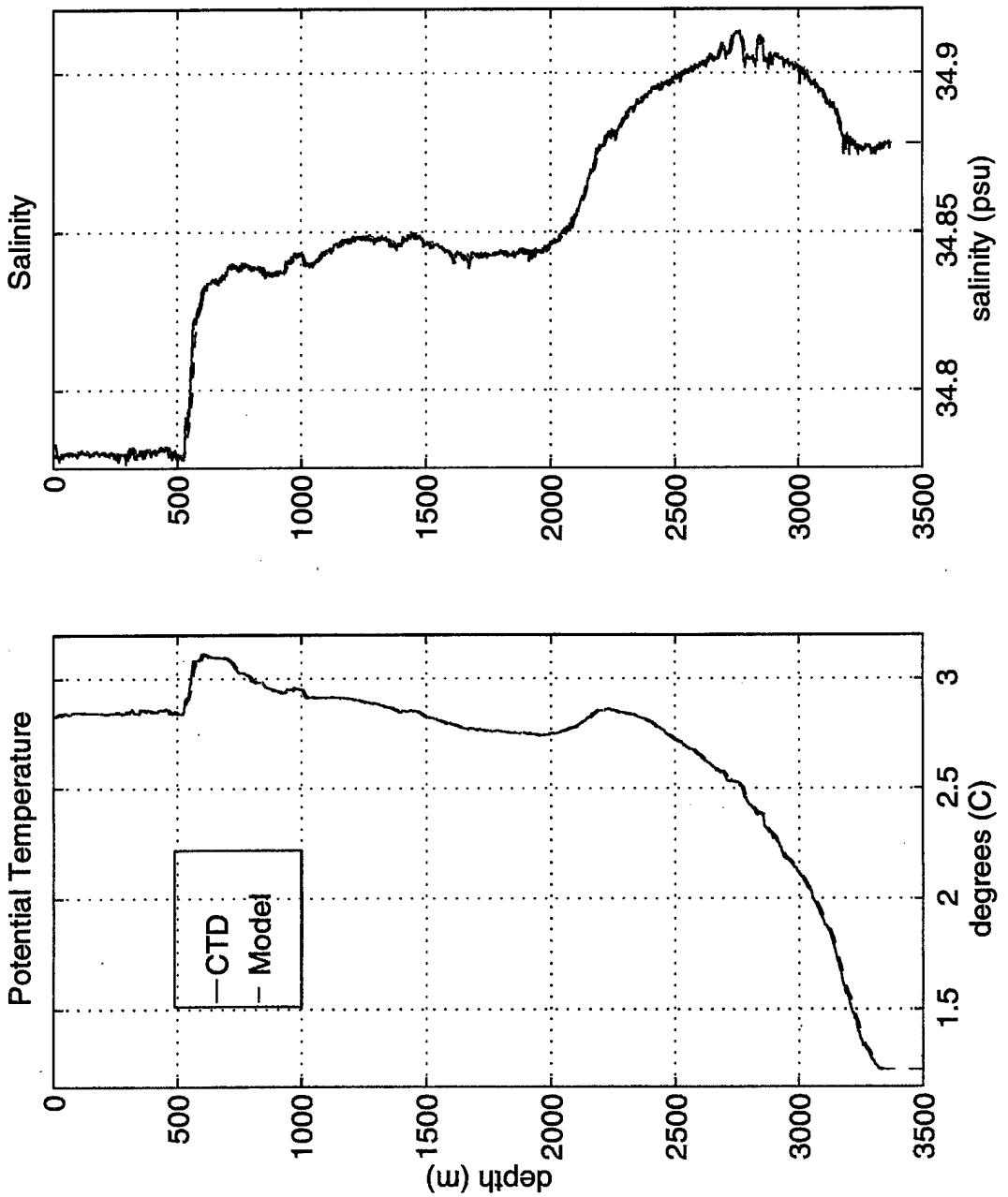

Figure 5.1: Observed potential temperature and salinity profiles for 12 February with corresponding model input data utilized for initialization of all model predictions. The salinity profiles have a linear correction applied.

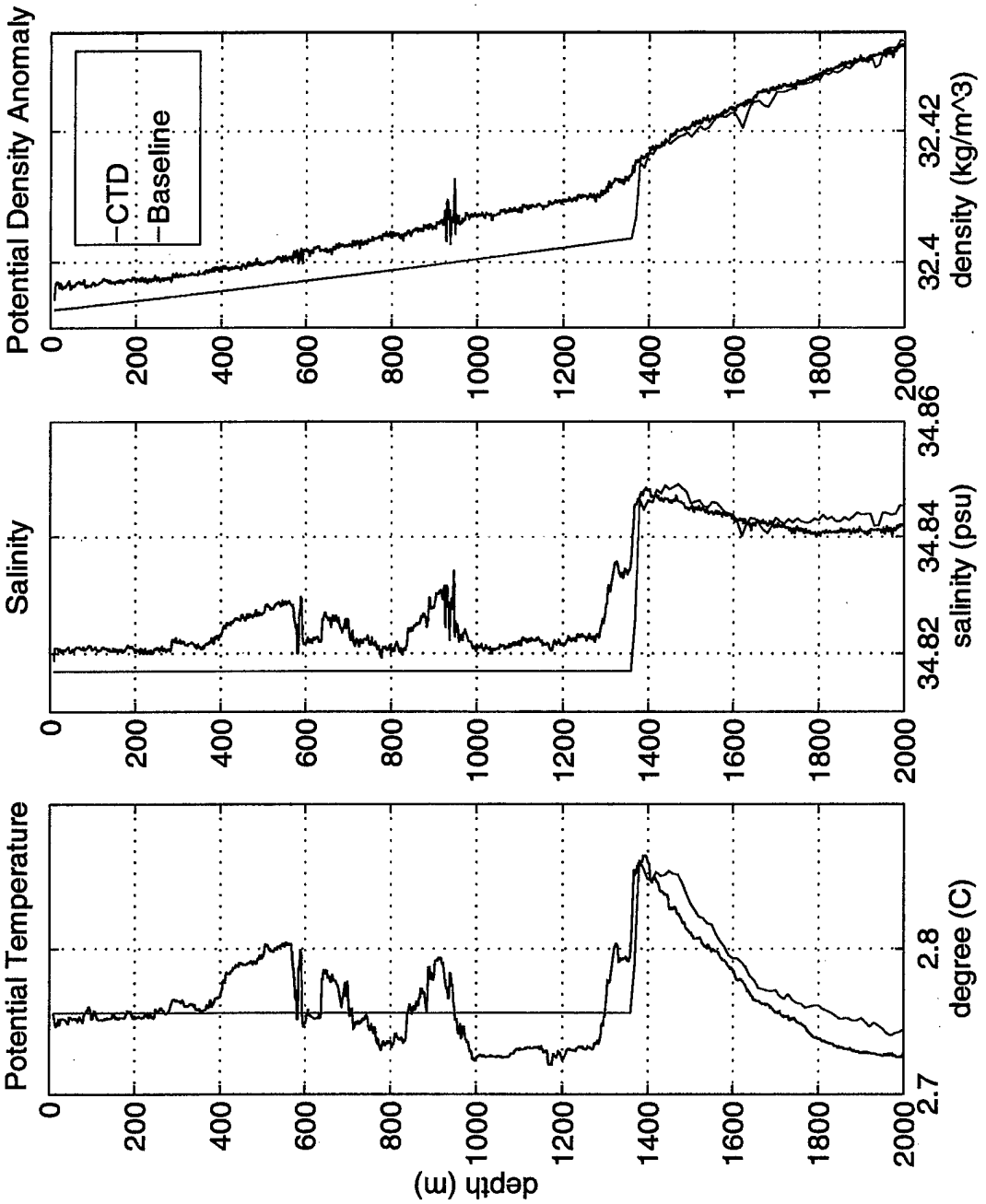

Figure 5.2: Model baseline predicted mixed layer potential temperature, salinity and potential density profiles compared with the observed profiles for 10 March. Model predicted mixed layer depth is 1361 m compared with an observed mixed layer depth of 1285 m.

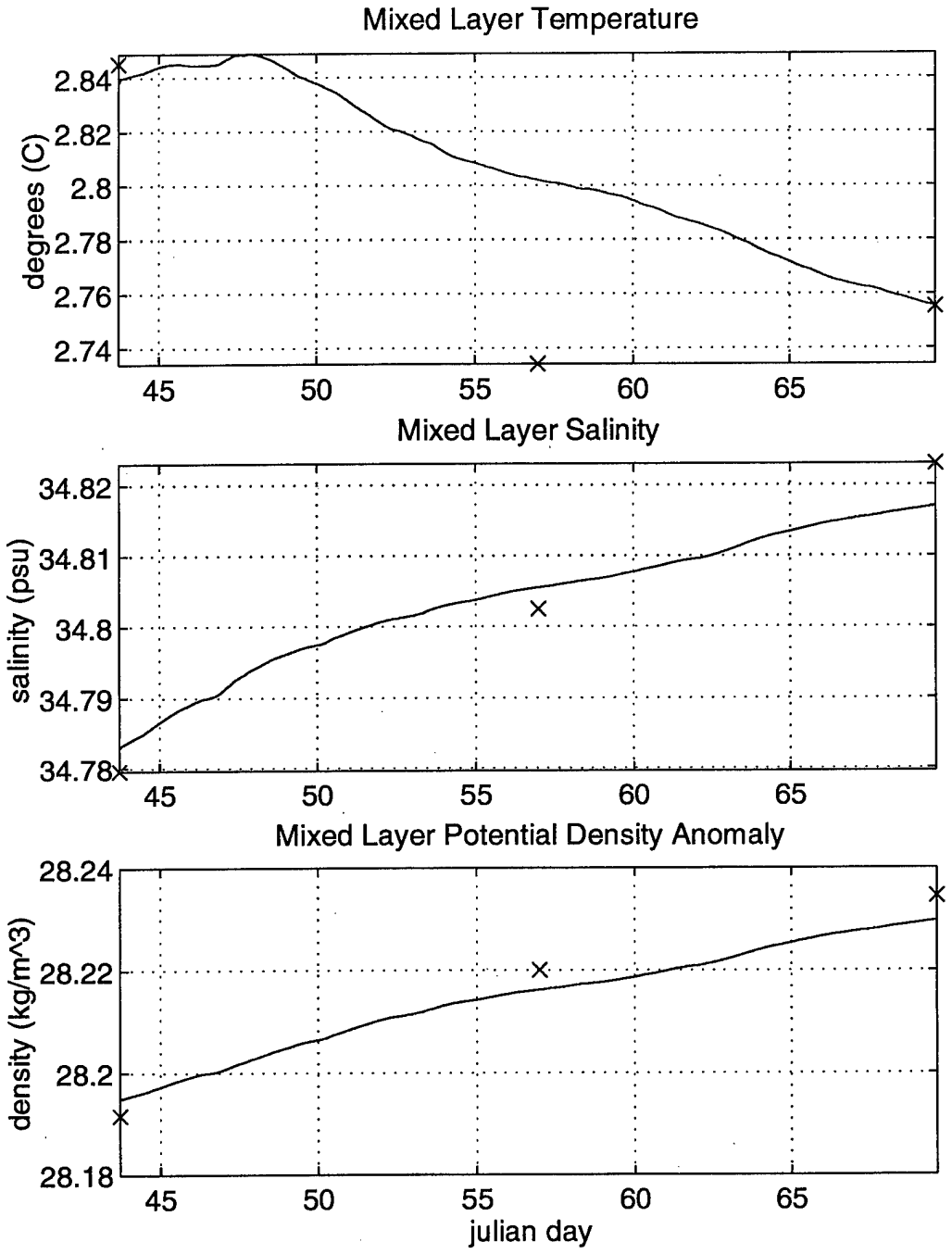

Figure 5.3: Time series of the baseline case compared to the observed mixed layer potential temperature, salinity and potential density for February 12 (day 43), February 25 (day 56) and March 10, 1997 (day 69). Although observed and predicted temperatures vary significantly near 25 February, potential density was well correlated.

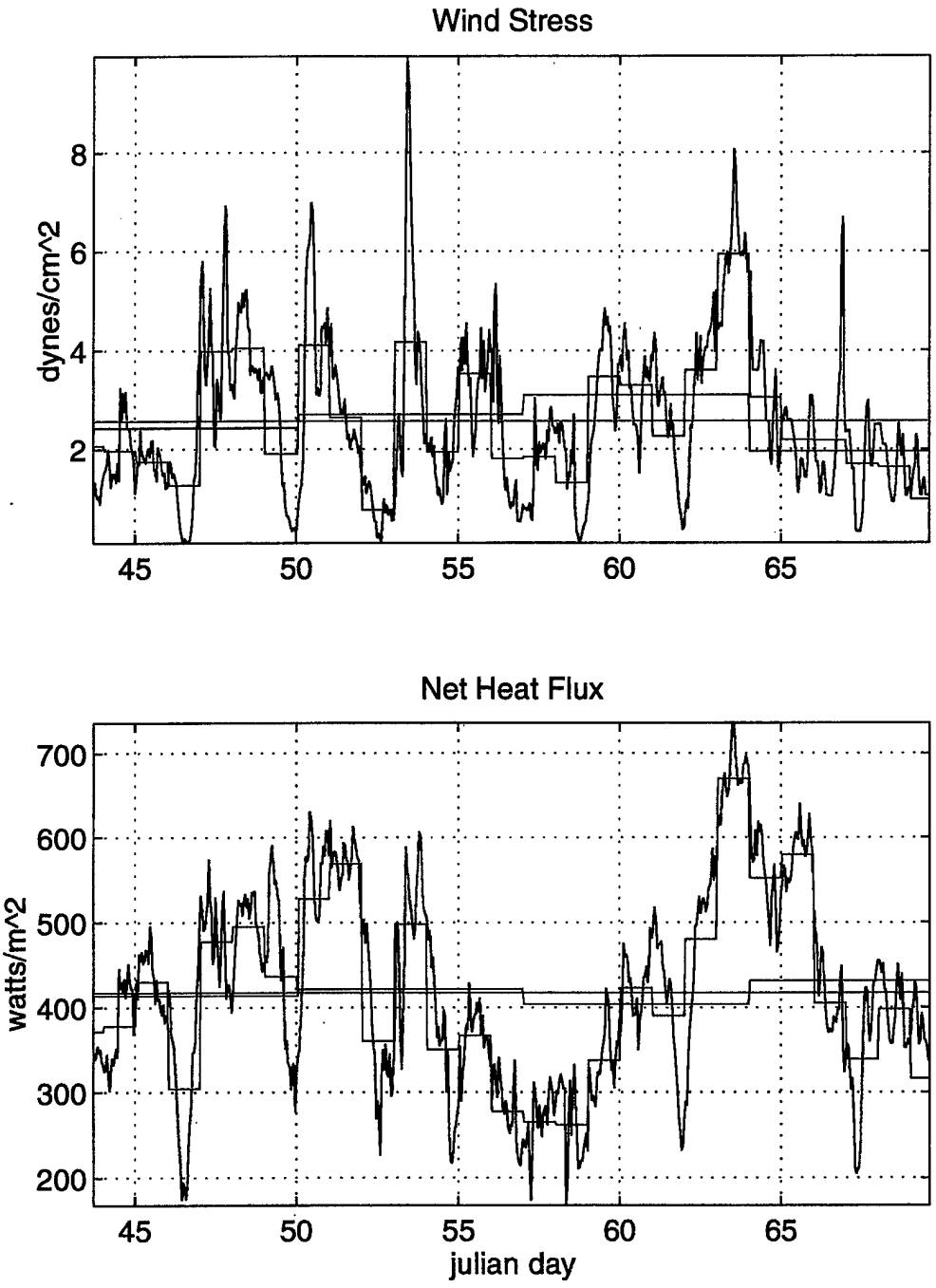

Figure 5.4: Time series of wind stress and net heat flux over the period showing the averaging interval variations of the input data. Data was averaged hourly (baseline case; black), daily (24 hours; red), weekly (7 days; blue) and constant forcing (entire period; green).

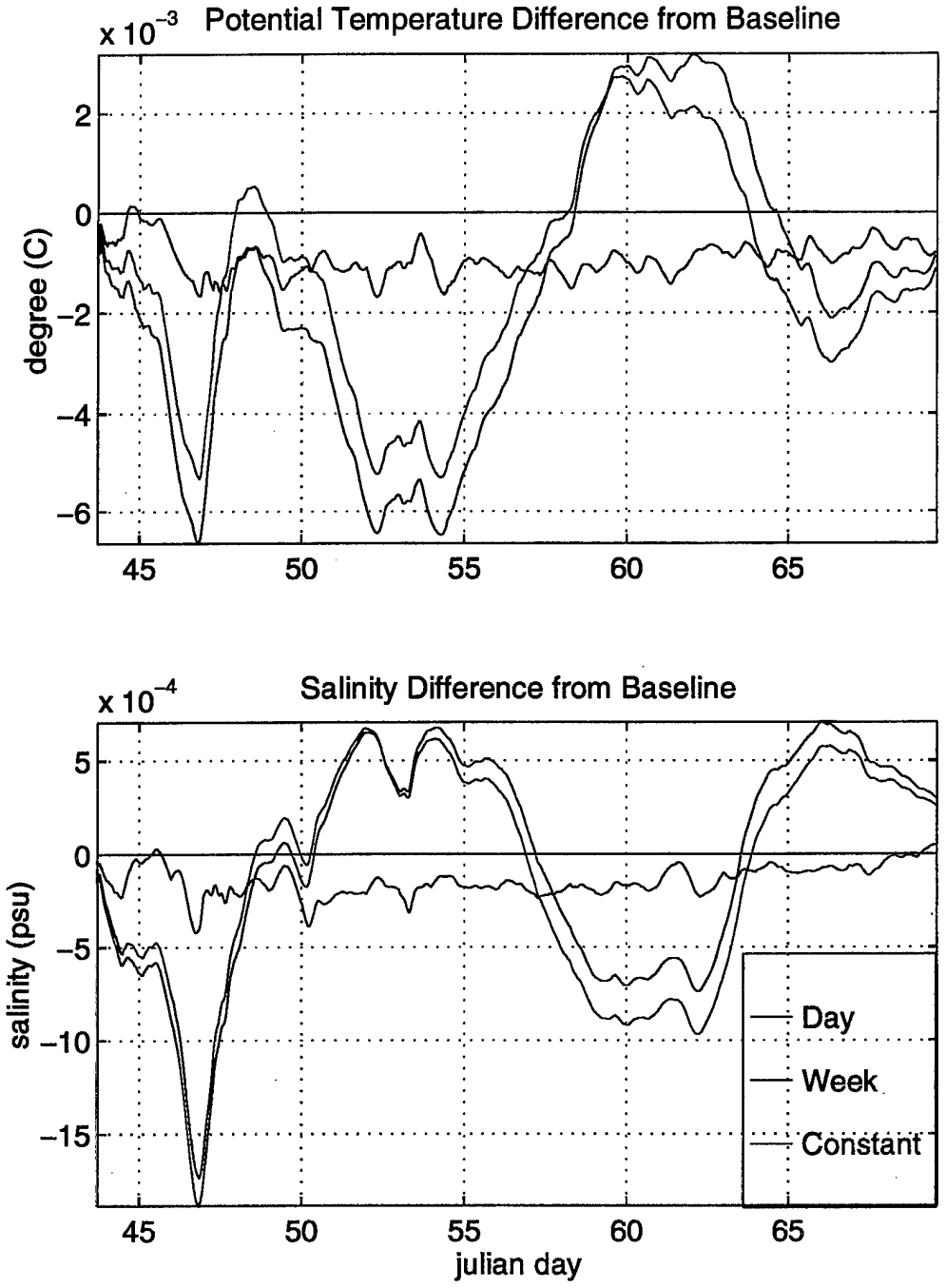

Figure 5.5: Time series comparing the potential temperature and salinity differences of the model averaging interval predictions from the baseline case. Final mixed layer temperature and salinity were barely affected by the fluctuating vs constant forcing.

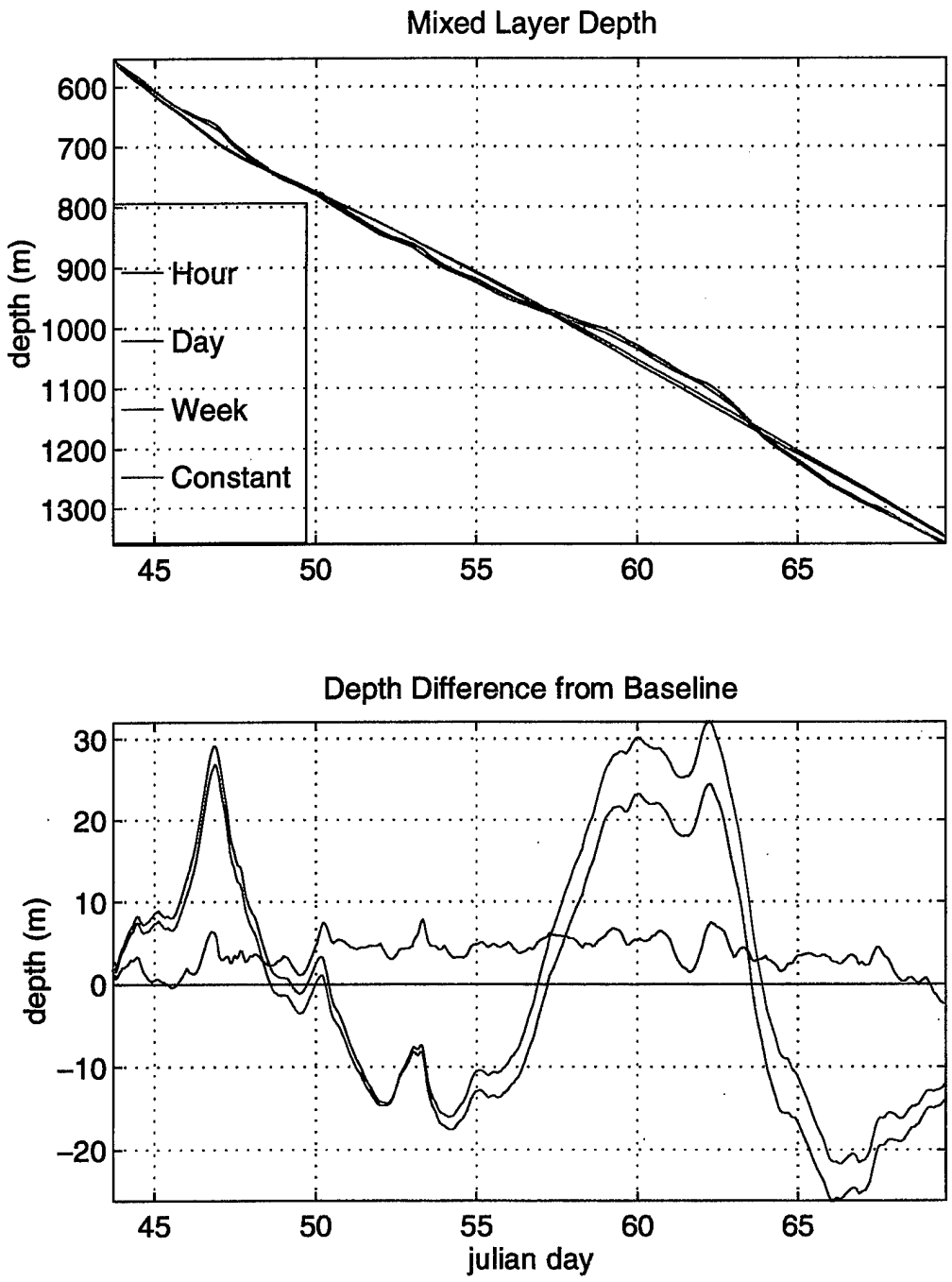

Figure 5.6: Time series of mixed layer depth and comparisons of the different averaging intervals to the baseline case. Only small changes were evident in the overall mixed layer depth as variations occurred where fluxes and wind stresses varied from the mean.

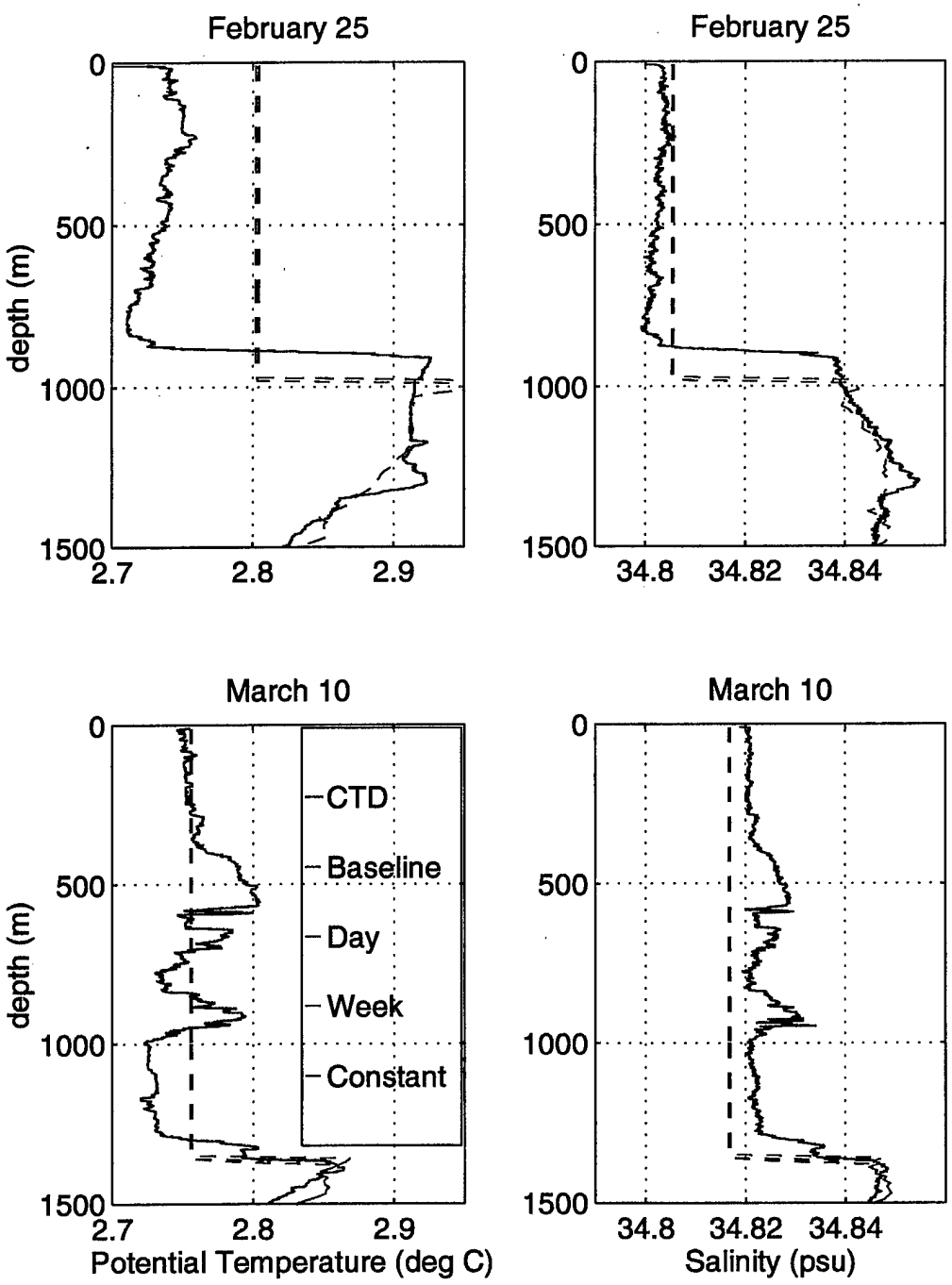

Figure 5.7: Observed potential temperature and salinity profiles compared with the different averaging interval model predicted mixed layer depths. Overall the averaging interval had little effect on the mixed layer temperature, salinity, or depth.

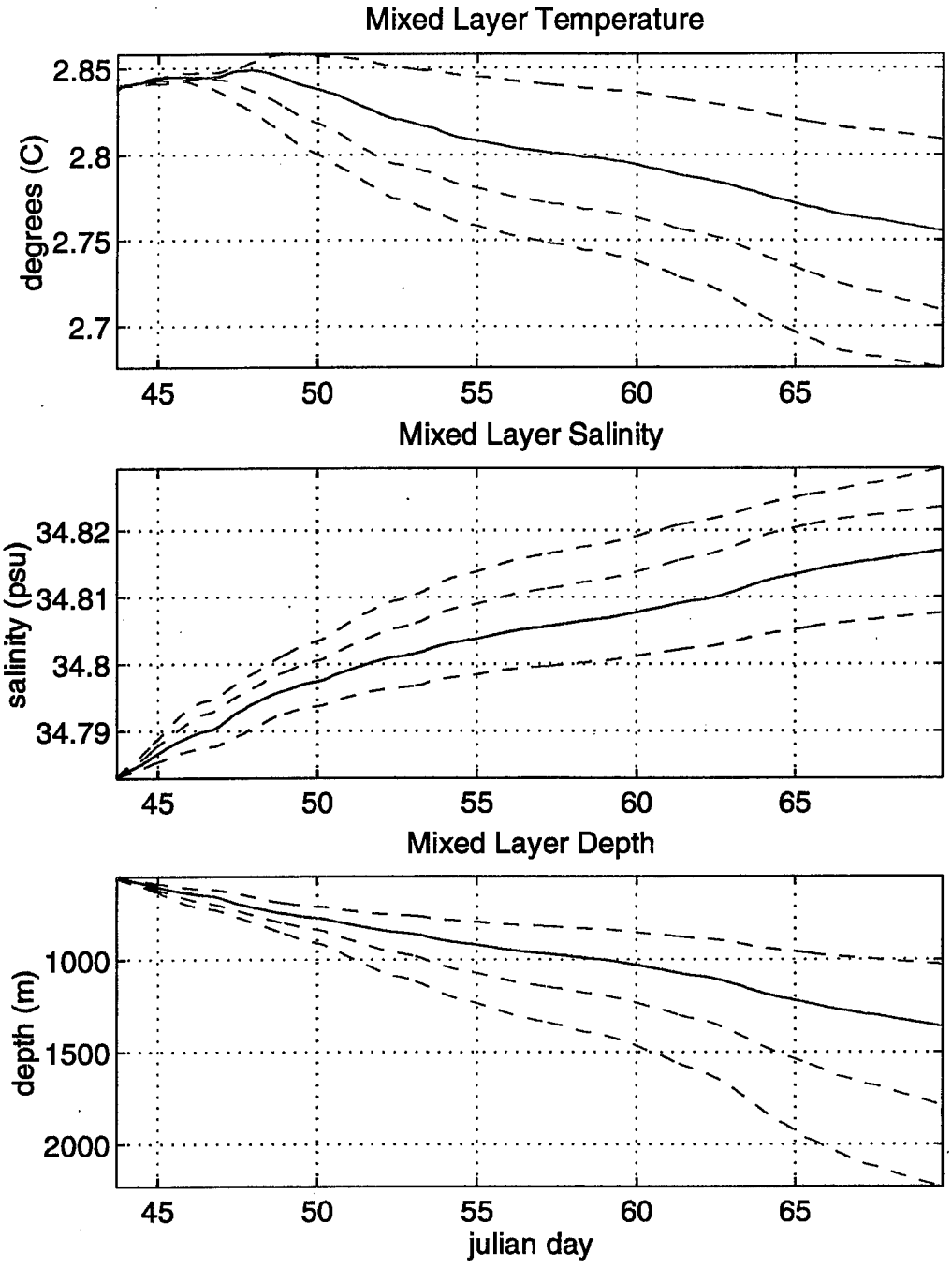

Figure 5.8: Time series of heat flux changes of - 50% (red), +50% (blue) and +100% (green). Model predicted mixed layer potential temperature, salinity and depth due to the respective heat flux changes are compared with the baseline case (black).

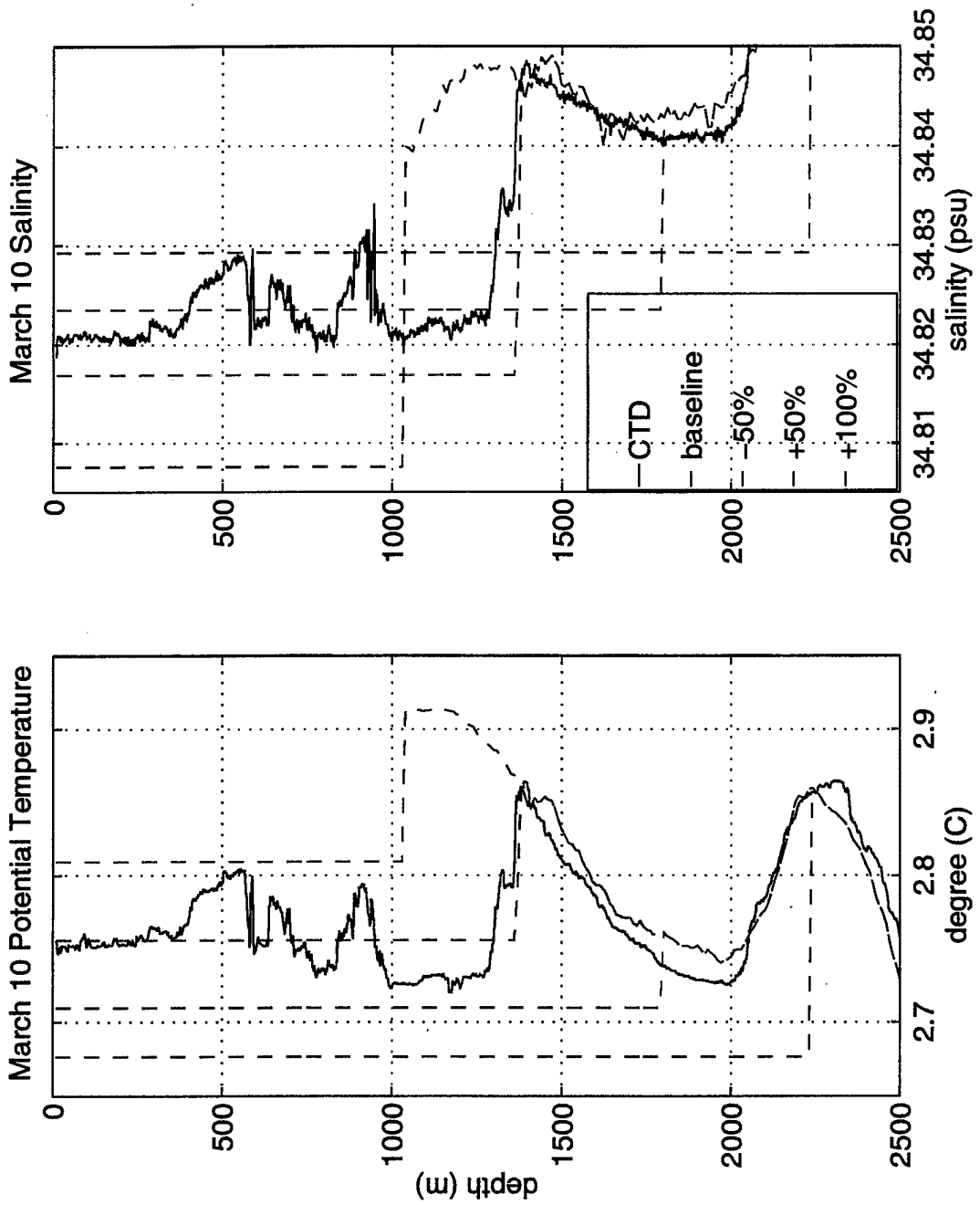

Figure 5.9: Observed potential temperature and salinity profiles of 10 March are compared with model predicted potential temperature and salinity profiles due to heat flux variations (-50%, +50% and +100%) and the baseline case.

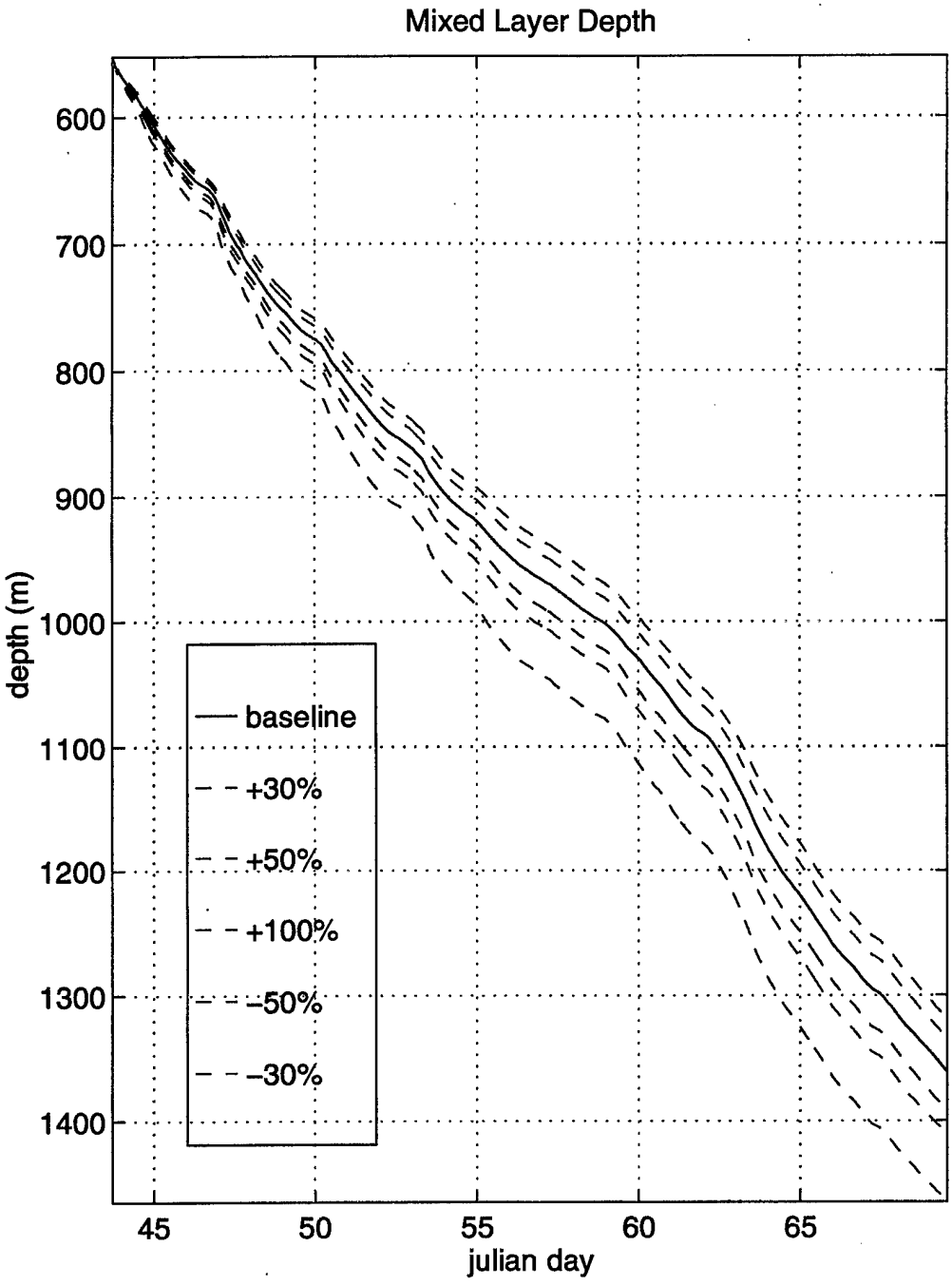

Figure 5.10: Time series of model predicted mixed layer depth due to wind stress variations (-30%, -50%, +30%, and +100%) compared with the baseline case. Little change to the mixed layer depth resulted from the wind stress variations.

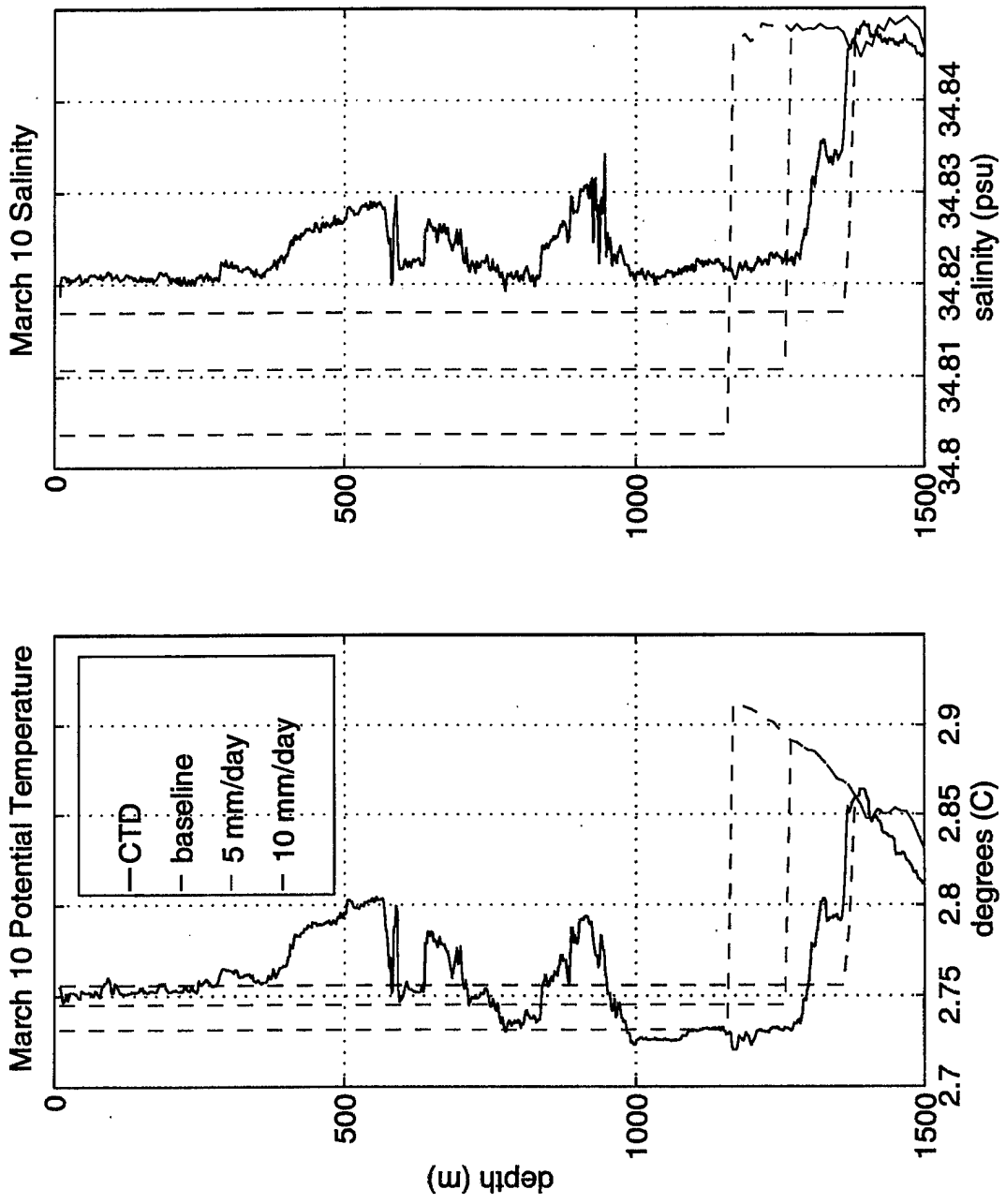

Figure 5.11: Observed potential temperature and salinity profiles of 10 March compared with precipitation variations (5mm/day and 10mm/day) and the baseline case. These variations had large effects on the mixed layer salinity and little effect on temperature.

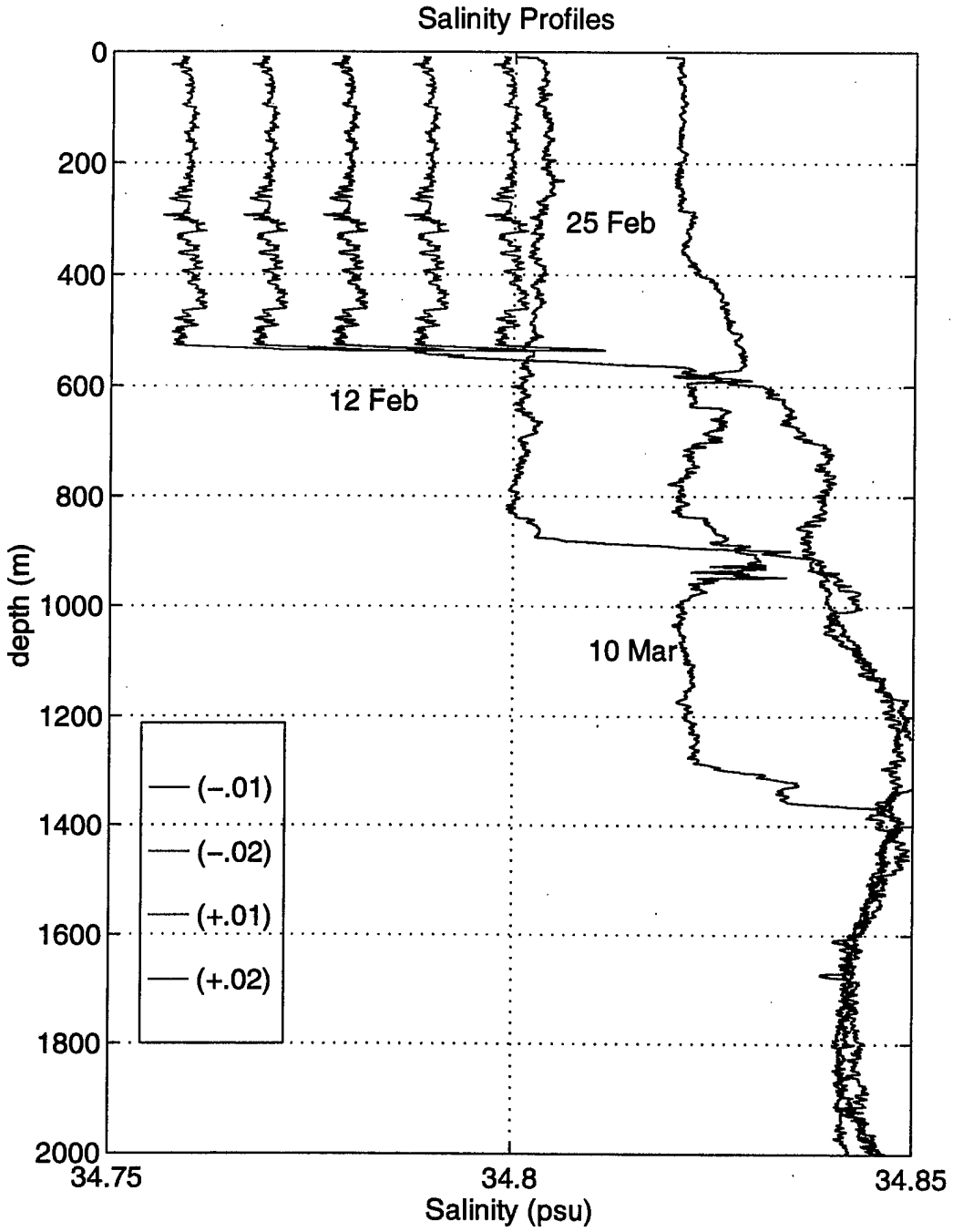

Figure 5.12: Mixed layer salinity variations were applied to the initial mixed layer salinity profile of 12 February. Model predictions were conducted offsetting the initial mixed layer salinity by (-) 0.02, (-) 0.01, (+) 0.01 and (+) 0.02 psu. Observed profiles are black.

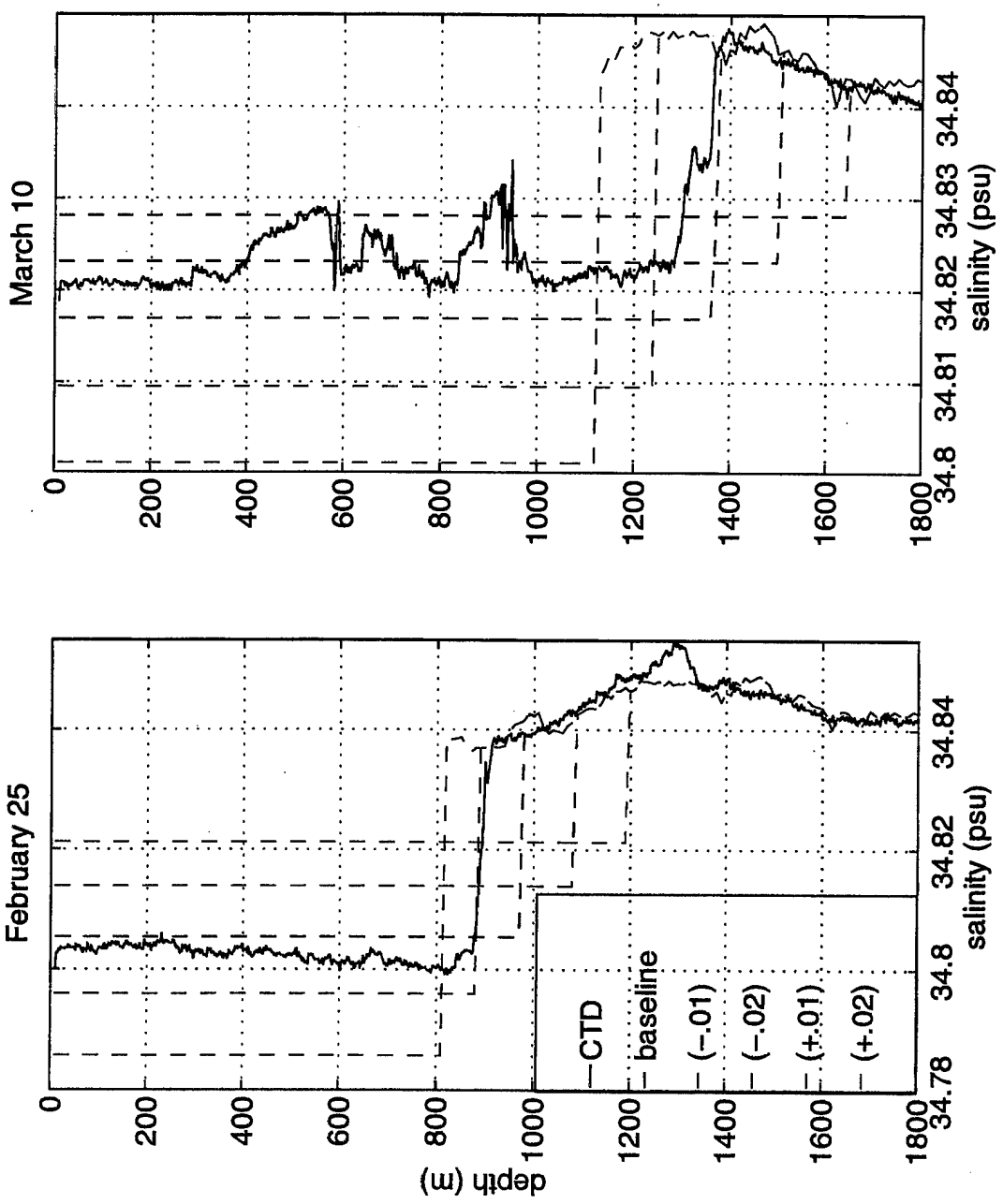

Figure 5.13: Observed salinity profiles for 25 February and 10 March compared with the baseline case and model predicted mixed layer salinity variations. Initial mixed layer salinity was offset (-) 0.02, (-) 0.01, (+) 0.01, and (+) 0.02 psu.

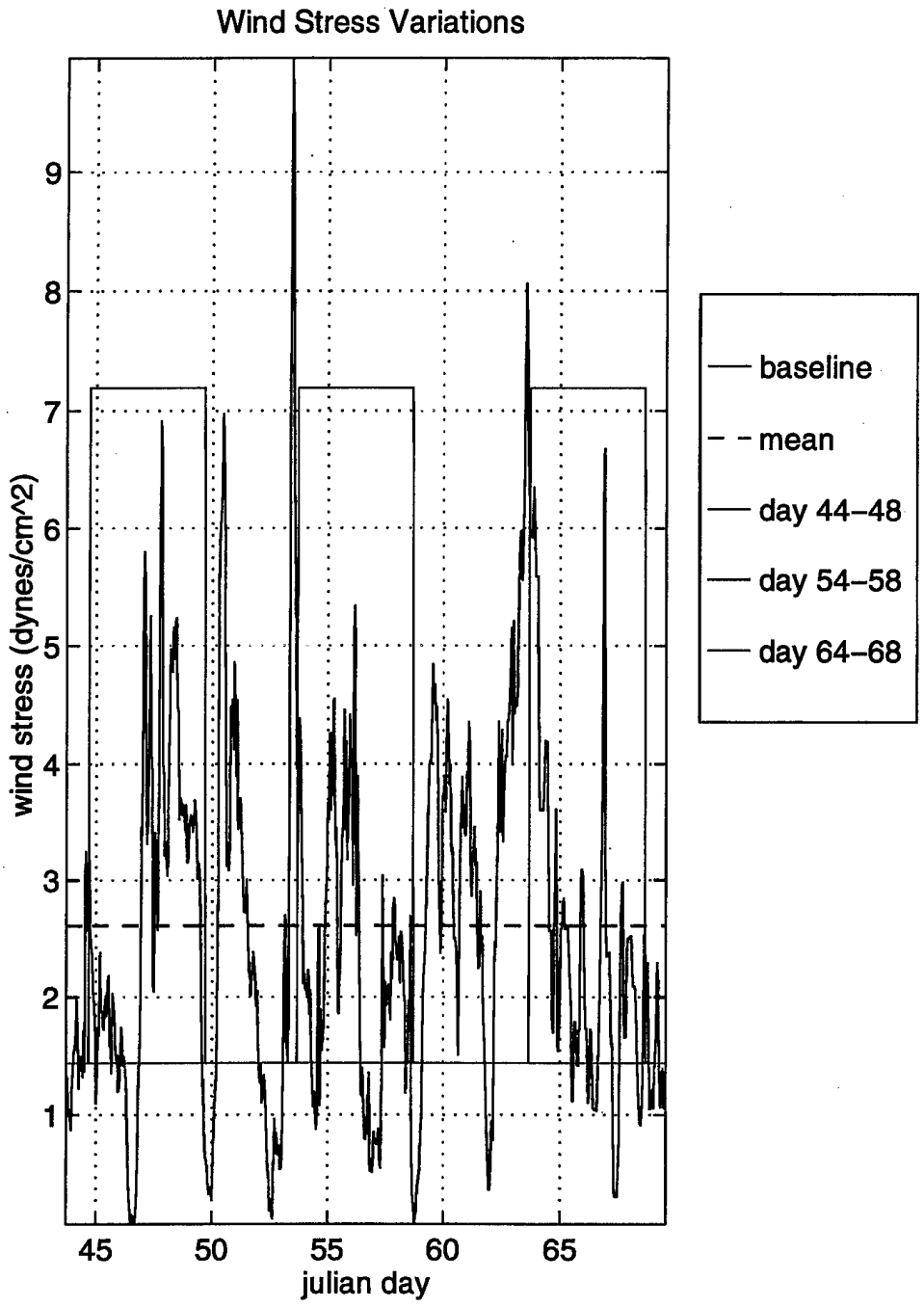

Figure 5.14: Time series of baseline and mean wind stress data, and superimposed are three 5 day storms (u_*^2 increased by 500%) at the beginning (days 44-48), middle (days 54-58) and end (days 64-68) periods. The overall mean wind stress was maintained.

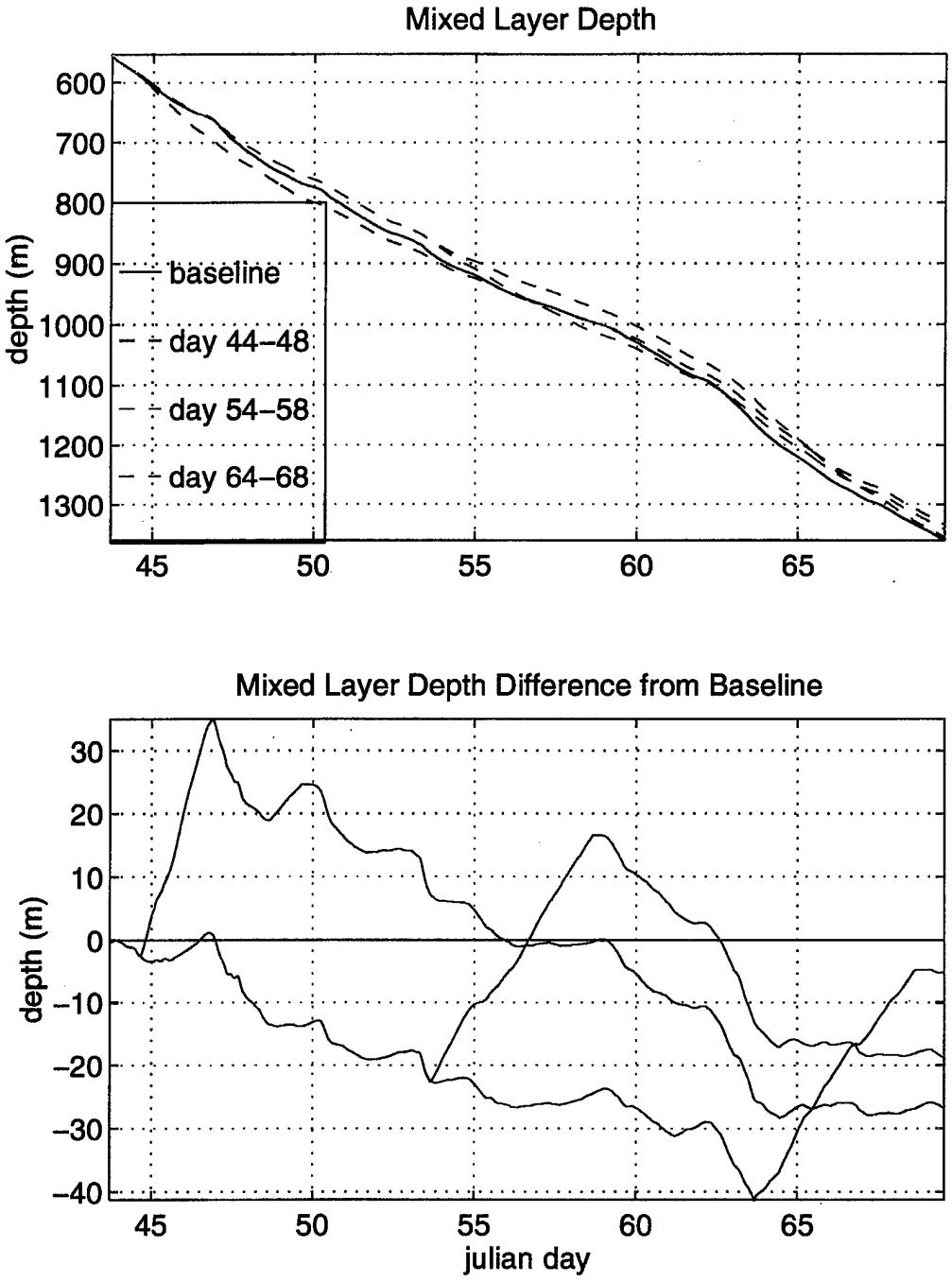

Figure 5.15: Time series of mixed layer depths and the mixed layer depth difference from the baseline case for the three individual storms. Time series show, the later the storm, the greater the model predicted mixed layer depth.

VI. SUMMARY AND CONCLUSIONS

A. SUMMARY

The first phase of the Labrador Sea Deep Convection Experiment was successfully completed onboard the R/V Knorr from February 2 to March 20, 1997 resulting in the most complete data set of atmospheric and oceanographic measurements ever collected in the Labrador Sea. With this information, application of the Naval Postgraduate School one dimensional ocean mixed layer model led to the prediction and verification of a deepened ocean mixed layer to almost 1300 m.

This study utilized Conductivity, temperature and depth (CTD) measurements of February 12, February 25 and March 10, 1997 at 57°N and 54°W to examine the mixed layer temperature, salinity and depth. A variety of air-sea interactions were analyzed to understand the effects of atmospheric forcing on the ocean mixed layer properties. In addition, integrated ocean heat and salt losses were calculated and compared to measured surface heat fluxes in an attempt to understand the mixed layer changes as active convection occurred. The strong surface heat fluxes and wind stresses present throughout the period were higher than climatological averages. Coincident with this strong forcing, the rate of mixed layer deepening was rapid.

Model integrations were conducted using parameters directly measured or derived from the atmospheric and oceanographic data including different averaging intervals. Model predicted mixed layer depth of the baseline case was only slightly greater than the observed value as the model predicted a mixed layer depth within 6% or 76 m of the measured mixed layer depth.

B. CONCLUSIONS

Several conclusions can be made about the conditions in the Labrador Sea during the winter of 1997 as observed mixed layer temperature, salinity and depth were compared with model profiles. The variations observed could be described by the following:

- Large scale advection: Without observation of advection, a basic assumption for application of the Naval Postgraduate School model is one dimensionality. It appears from the CTD data measured and analyzed that this was not the simple one dimensional case assumed at the onset. Although CTD profiles show consistent deep water mass properties, some of the mixed layer changes and inconsistencies appear to be due to significant movement of the surface waters. It is believed that the CTD casts, although measured in the same location, were actually measuring different water masses.

- Small scale advection: Advection was neglected during these model integrations but it is likely that small scale features affected the observation. During the cruise, it was noted that up-cast CTD profiles would often differ significantly from the downcast. This suggests the likelihood of intrusions of warmer, saltier water in the mixed layer. Without exact knowledge of the origin of these intrusions, accurate model prediction becomes more difficult and could cause variations in the predicted mixed layer depths.

- Model parameterization: The NPS one dimensional mixed layer model was first designed for use in the shallow mixed layer waters of the Pacific Ocean where tuning coefficients were specifically determined for that area. Applying the model to an area of very deep convection which has significantly different conditions may require localized tuning. The determination of the tuning coefficients is a study within itself. Model parameterization with more specialized tuning coefficients could lead to a more accurate model.

- Data collection: All surface data was collected onboard the R/V Knorr which was moving throughout the Labrador Sea during the period. Conditions at the CTD locations could have been different from those onboard the ship leading to errors in the derived forcing for the model.

The following conclusions can be made for the many model integrations conducted and the effect of the various parameters on the ocean mixed layer of the Labrador Sea:

- Model: The NPS one dimensional model worked well. Although the one dimensional assumption was not perfect, it was close enough to simulate most of the physics occurring.

- Integrated heat and salt loss: A patch of cold, low salinity water was observed in the mid period measurements but final temperatures were well predicted. It is assumed that surface heat fluxes controlled the large difference in temperature rather than errors simply counteracting each other. Although the salinity

difference cannot be explained by the surface forcing of precipitation minus evaporation, this was not crucial in terms of the overall density which was well compensated.

- Data averaging interval (fluctuating vs constant forcing): Model predictions showed that the averaging interval of input data was not crucial to the mixed layer depth. Data averaged over one month gave results within 15 m of the baseline (hourly averaged) case. The longer averaging period appeared to only have an overall small 'linear' effect.

- Sensitivity analysis: Model predictions showed that heat flux variations had the most significant effect on the mixed layer depth. Both positive and negative changes caused significant changes to the mixed layer temperature, salinity and depth.

- Wind stress: Model predictions indicated that wind stress variations were not extremely important in the long run. Large changes to the wind stress only caused small variations to the mixed layer depth.

- Precipitation: Model predictions showed that precipitation is important to the structure of the mixed layer, but variations are not a dominant factor in the mixed layer depth.

- Salinity variations: Model predictions showed that although mixed layer salinity variations can affect the mixed layer depth, offset values chosen caused unrealistic results.

- Deepened mixing to 2000 m: Model predictions showed that enhanced deepening would be likely in a cold winter. Baroclinic instabilities or some other special mechanism is not needed for deepened convection. If December to January conditions had strong atmospheric forcing similar to February and March forcing, mixing could easily have reached 2000 m.

- Storm variations: Model predictions showed that individual storms were not important for direct mixing in the long run as a constant wind stress was more effective at mixing for the same mean wind stress. The later storms were slightly more effective than storms at the beginning.

Despite potential problems, the density field appeared to be reasonably one dimensional, and the model appeared to simulate conditions in the central Labrador Sea quite well for the winter of 1997. These positive results suggest the feasibility of future modeling of ocean mixed layers and deepened convection not only for the Labrador but other polar seas.

C. RECOMMENDATIONS

The Labrador Sea Deep Convection Experiment continues as another at sea period is planned for the winter of 1998. Questions or concerns which could immediately give more insight on this next phase include:

- Advection or currents: It is essential to determine whether the CTD casts at the same location were from the same surface water mass. Drifters indicate motion of 200 - 250 km in the short 26 days of deepened convection. Finding CTDs for comparisons in different locations but of the same water mass could resolve some of the inconsistencies in the calculations explaining why the integrated heat and salt loss varied so much when compared to measured values.

- Large-eddy simulation (LES): Although not a true one dimensional case, the one dimensional ocean mixed layer model did explain the physics occurring in the Labrador Sea during a deep convection event. A better understanding and confirmation could occur by comparing these results to similar LES model applications. In addition, the LES model could be used to tune the NPS mixed layer model.

APPENDIX. DATA

Listed below are most symbols utilized in the various equations in this thesis. Units and constants with their corresponding values are listed where appropriate.

SYMBOL	DEFINITION
α	thermal expansion coefficient ($.25 \times 10^{-3}$/°C)
β	salinity expansion coefficient ($.8 \times 10^{-3}$/ppm)
L	latent heat of vaporization (2.5×10^{6} J/kg)
g	gravitational acceleration (9.81 m/s)
ϵ	viscous dissipation
E	total turbulent kinetic energy
ρ	seawater density (kg/m^3)
ρ_{air}	atmospheric density (1.25 kg/m^3)
ρ_o	reference sea water density (kg/m^3)
w_e	entrainment velocity (m/s)
Q_o	net surface heat flux (watt/m^2)
c_p	seawater specific heat capacity (4186 J/kg°C)
c_{pa}	specific heat of air at constant pressure (J/kg°C)
E	evaporation (m/s)
P	precipitation (m/s)
ϵ_1	fractional difference between S_{water} and S_{ice} if $S_{ice} = 0$ $\epsilon_1 = 1$; if $S_{ice} = S_{water}$ $\epsilon_1 = 0$ (dimensionless)
μ	melting rate of ice (m/s)
F	freezing rate of ice (m/s)
h	mixed layer depth (m)

SYMBOL	DEFINITION
u_*	friction velocity (m/s)
τ	wind stress at sea surface (dynes/cm^2)
c_D	drag coefficient (dimensionless)
u	mean wind speed at reference height (m/s)
c_T	heat flux coefficient (dimensionless)
q_{sfc}	specific humidity mixing ratio of water vapor in saturated air at surface temperature (g/kg)
q	specific humidity mixing ratio of water vapor in saturated air at measurement height (g/kg)
c_E	evaporation coefficient (dimensionless)
T_{sfc}	bulk or surface water temperature (°C)
θ	potential temperature of air at reference height (°C)
Q	total heat transferred (watt/m^2)
Q_H	surface heat flux (watt/m^2)
Q_E	rate of evaporation from surface (watt/m^2)

LIST OF REFERENCES

Broecker, W. S. and T. H. Peng, 1982: *Tracers in the sea*, Eldigio Press, 690 pp.

Bunker, A. F. and L. V. Worthington, 1976: Energy exchange charts of the North Atlantic Ocean. *Bull. Amer. Meteorol Soc., 57*, 670-678.

Charnock, H., 1955: Wind stress on a water surface. *Q.J.R. Meteorol. Soc., 81*, 639-640.

Clarke, R. A. and J. C. Gascard, 1983: The formation of Labrador Sea Water. Part I: Large-scale processes, *J. Phys.Oceanogr., 13*, 1764 -1778.

Curry, R. G., and M. S. McCartney, 1996: Labrador Sea Water carries northern climate signal south, *Oceans, 39(2)*, 24-28.

Fairbridge R. W., 1966: *Encyclopedia of Earth Sciences*, Vol. 1, *The Encyclopedia of Oceanography*, Reinhold Publishing Corporation, 1012 pp.

Garwood, R. W., Jr., 1977: An oceanic mixed layer model capable of simulating cyclic states, *J. Phys. Oceanogr., 7*, 455-468.

Garwood, R. W., Jr., 1991: Enhancements to deep turbulent entrainment, In Deep Convection and Deep Water Formation in the Ocean, ed., P. C. Chu and J. C. Gascard, Elsevier, 189-205.

Garwood, R. W., Jr., P. Muller, and P.C. Gallacher, 1985: Wind direction and equilibrium mixed layer depth in the tropical Pacific Ocean, *J. Phys. Oceanogr., 15*, 1332-1338.

Gascard, J. C., 1990: Deep convection and deep water formation: Progress and directions, *EOS, 71*, 1837-1839.

Killworth, P. D., 1983: Deep convection in the world ocean. *Rev. Geophys. and Space Phys., 21(1)*, 1-26.

Kraus, E. B. and J. A. Businger, 1994: *Atmosphere-Ocean Interaction*. Vol. 2, Oxford Monographs on Geology and Geophysics No. 27. Oxford University Press, 362 pp.

Lazier, J. R. N. and D. G. Wright, 1993: Annual velocity variations in the Labrador Current, *J. Phys. Oceanogr., 23*, 659-678.

Lazier, J. R., 1980: Oceanographic conditions at ocean weather ship Bravo 1964-1974, *Atmos.Ocean*, *18*, 227-238.

Livezey, M., 1988: Discrete precipitation effects on seasonal mixed layer dynamics in the northern Pacific Ocean, M.S. thesis, Naval Postgraduate School, 71 pp.

Pickard, G. L. and W. J. Emery, 1990: *Descriptive physical oceanography: an introduction*, Pergamon Press, 320 pp.

Schmitt, R. W., 1996: If rain falls on the ocean - does it make a sound? Fresh water's effect on ocean phenomena. *Oceans*, *39(2)*, 4-8.

Schmitz, W. J. and M. S. McCartney, 1993: On the north Atlantic circulation. *Revs. of Geophys.*, *31*, 29-49.

Smith, S. D., 1988: Coefficients for sea surface wind stress, heat flux, and wind profiles as a function of wind speed and temperature, *J. Geophys. Res.*, *93*, 15267-15472.

INITIAL DISTRIBUTION LIST

No. Copies

1. Defense Technical Information Center 2
   8725 John J. Kingman Rd., STE 0944
   Ft. Belvoir, VA 22060-6218

2. Dudley Knox Library 2
   Naval Postgraduate School
   411 Dyer Rd.
   Monterey, CA 93943-5101

3. Chairman (Code OC/BF) 1
   Department of Oceanography
   Naval Postgraduate School
   Monterey, CA 93943-5101

4. Chairman (Code MR/Wx) 1
   Department of Meteorology
   Naval Postgraduate School
   Monterey, CA 93943-5101

5. Prof. Roland W. Garwood (Code OC/Gd) 2
   Department of Oceanography
   Naval Postgraduate School
   Monterey, CA 93943-5101

6. Prof. Peter S. Guest (Code MR/Gs) 2
   Department of Meteorology
   Naval Postgraduate School
   Monterey, CA 93943-5101

7. Dr. Thomas B. Curtin 1
   Office of Naval Research (Code 3220M)
   800 North Quincy Street
   Ballston Tower One
   Arlington, VA 22217-5660

8. Dr. Manuel Fiadeiro 1
Office of Naval Research (Code 3220M)
800 North Quincy Street
Ballston Tower One
Arlington, VA 22217-5660

9. Dr. Randy Jacobson. 1
Office of Naval Research (Code 322HL)
800 North Quincy Street
Ballston Tower One
Arlington, VA 22217-5660

10. Dr. Clayton Paulson. 1
Office of Naval Research (Code 322HL)
800 North Quincy Street
Ballston Tower One
Arlington, VA 22217-5660

11. LCDR Laura Bramson. 1
Naval European Meteorology and Oceanography Center
PSC 819 Box 31
FPO AE 09645-3200